

PREDICTIVE ONLINE OPTIMISATION WITH APPLICATIONS TO OPTICAL FLOW

Tuomo Valkonen*

Abstract Online optimisation revolves around new data being introduced into a problem while it is still being solved; think of deep learning as more training samples become available. We adapt the idea to dynamic inverse problems such as video processing with optical flow. We introduce a corresponding *predictive online primal-dual proximal splitting* method. The video frames now *exactly correspond to the algorithm iterations*. A user-prescribed predictor describes the evolution of the primal variable. To prove convergence we need a predictor for the dual variable based on (proximal) gradient flow. This affects the model that the method asymptotically minimises. We show that for inverse problems the effect is, essentially, to construct a new dynamic regulariser based on infimal convolution of the static regularisers with the temporal coupling. We develop regularisation theory for dynamic inverse problems, and show the convergence of the algorithmic solutions in terms of this theory. We finish by demonstrating excellent real-time performance of our method in computational image stabilisation.

1 INTRODUCTION

On Hilbert spaces X_k and Y_k , ($k \in \mathbb{N}$), consider the formal problem

$$(1.1) \quad \min_{x^1, x^2, \dots} \sum_{k=1}^{\infty} F_k(x^k) + G_k(K_k x^k) \quad \text{s.t.} \quad x^{k+1} = \bar{A}_k(x^k),$$

where $F_k : X_k \rightarrow \overline{\mathbb{R}}$ and $G_k : Y_k \rightarrow \overline{\mathbb{R}}$ are convex, proper, and lower semicontinuous, $K_k \in \mathbb{L}(X_k; Y_k)$ is linear and bounded, and the *temporal coupling* operators $\bar{A}_k : X_k \rightarrow X_{k+1}$. This problem is clearly challenging; even its solutions are generally well-defined only asymptotically.

Instead of trying to solve (1.1) exactly, what if we take only *one step* of an optimisation algorithm on each partial problem

$$(1.2) \quad \min_{x^k \in X_k} J_k(x_k) := F_k(x^k) + G_k(K_k x^k),$$

and use an approximation $A_k : X_k \rightarrow X_{k+1}$ of the possibly unknown \bar{A}_k to predict between the steps? Can we obtain convergence in an asymptotic sense, and to what? We set out to study these questions, in particular to develop a predictive “online” primal-dual method.

Our simple model problem is image sequence denoising: we are given noisy images $\{b^k\}_{k \in \mathbb{N}} \subset X = L^2(\Omega)$ and bijective displacement fields $v^k : X \rightarrow X$ such that the images roughly satisfy the *optical*

This research has been supported by Escuela Politécnica Nacional internal grant PIJ-18-03 and Academy of Finland grants 314701 and 320022.

*Department of Mathematics and Statistics, University of Helsinki, Finland *and* ModeMat, Escuela Politécnica Nacional, Quito, Ecuador, tuomo.valkonen@iki.fi, ORCID: [0000-0001-6683-3572](https://orcid.org/0000-0001-6683-3572)

flow constraint $b^{k+1} \approx A_k(b^k)$ for $A_k(x) := x \circ v^k$. For an introduction to optical flow, we refer to [5]. The static problem (1.2) is the isotropic total variation denoising

$$(1.3) \quad \min_{x \in X} \frac{1}{2} \|x - b^k\|_X^2 + \alpha \|Dx\|_{\mathcal{M}},$$

where $\alpha > 0$ is a regularisation parameter and D a measure-valued differential operator. In the dynamic case we would like the approximate solutions $\{x^k\}_{k \in \mathbb{N}}$ to also satisfy $x^{k+1} \approx A_k(x^k)$. In principle, we could for the first N frames for some penalisation parameter $\beta > 0$ solve

$$\min_{x^1, \dots, x^{N+1} \in X} \sum_{k=0}^N \left(\frac{1}{2} \|x^k - b^k\|_X^2 + \alpha \|Dx^k\|_{\mathcal{M}} + \frac{\beta}{2} \|x^{k+1} - A_k(x^k)\|_X^2 \right),$$

or a version that linearises A_k . However, when the number of frames N is high, these problems become numerically increasingly challenging. Also, if we want to solve the problem for $N + 1$ frames, we may need to do the same amount of work again, depending on how well our algorithm can “restart”. Primal-dual methods in particular tend to be very sensitive to initialisation.

An alternative is to try to solve the problem in an “online” fashion, building the gradually changing data into the algorithm design [40]. We refer to [19, 6, 27] for introductions and further references to online methods in machine learning. Online Newton methods have also been studied for smooth PDE-constrained optimisation [8, 17]. Our approach has more in common with machine learning and nonsmooth optimisation. From this point of view, basic online methods seek a low *regret* for a dynamic solution sequence compared to a fixed solution. With the notation $x^{1:N} := (x^1, \dots, x^N)$, for any $B \subset X$,

$$\text{regret}_B(x^{1:N}) := \sup_{\bar{x} \in B} \sum_{k=1}^N \left(J_k(x^k) - J_k(\bar{x}) \right).$$

This does not model the temporal nature of our true solutions. In [18] a form of *dynamic regret* is introduced. Given a comparison set $\mathcal{B}_{1:N} \subset \prod_{k=1}^N X_k$ of possible true solutions, it reads

$$(1.4) \quad \text{dynamic_regret}_{\mathcal{B}_{1:N}}(x^{1:N}) := \sup_{\bar{x}^{1:N} \in \mathcal{B}_{1:N}} \sum_{k=1}^N \left(J_k(x^k) - J_k(\bar{x}^k) \right).$$

We can, for example, for $\mathcal{B}_0 \subset X_0$ and true temporal coupling operators $\bar{A}_k : X_k \rightarrow X_{k+1}$ take

$$(1.5) \quad \mathcal{B}_{1:N} = \{(\bar{x}^1, \bar{x}^2, \dots) \mid \bar{x}^0 \in \mathcal{B}_0, \bar{x}^{k+1} = \bar{A}_k(\bar{x}^k), k \geq 0\}.$$

The idea now would be to obtain a low dynamic regret by some strategy. One possibility is what we have already mentioned: take one step of an optimisation method towards a minimiser of each J_k , and then use A_k to predict an approximate solution for the next problem. Repeat. In this approach, the new data frames exactly correspond to algorithm iterations. The strategy of very inexact solutions is motivated by the fact that neural networks can be effective—not get stuck in local optima—exactly because subproblems are not solved exactly [9]. Another type of applications is studied in [2, 29], where new data can only be sampled intermittently, and the algorithm is let to run several steps between the samplings.

In Section 3 we show that a predictive forward-backward splitting obtains low dynamic regret, in line with similar results in the literature [18, 38]. This treatment serves as an introduction of concepts and ideas for our main interest: primal-dual methods. Indeed, forward-backward splitting is poorly applicable to (1.3): the proximal step is just as expensive as the original problem. Therefore, it is usually applied to the Fenchel–Rockafellar dual, on which it is effective. However, we are given a primal predictor A_k , so dual formulations are not directly applicable. Moreover, purely dual formulations are

not feasible for deblurring and more complex inverse problems. A solution is to work with primal-dual formulations of the static problems (1.2),

$$(1.6) \quad \min_{x \in X_k} \max_{y \in Y_k} F_k(x) + \langle K_k x, y \rangle - G_k^*(y).$$

Here G_k^* is the Fenchel conjugate of G_k . A popular method for this type of problems is the *primal-dual proximal splitting* (PDPS) of Chambolle and Pock [11]. We refer to [34] for an overview of different variants, alternatives, and extensions to non-convex problems.

MAIN CONTRIBUTIONS

We develop in Section 5 a predictive online PDPS for (1.1). For the primal variable we use the user-prescribed predictor $A_k : X_k \rightarrow X_{k+1}$, but for the dual variable we need to construct a more technical predictor, imposed by the convergence (regret) theory. This forms the main challenge of our work. To prepare for this, we introduce and interpret in Section 4 appropriate *partial primal gap* functionals that we will use to replace the dynamic regret (1.4), not applicable to primal-dual methods.

Finally, since we do not solve (1.2) exactly, for inverse problems such as (1.3) our optimisation method forms a *regularisation method* [15]. We develop an approach to study the corresponding asymptotic properties in Section 6. We finish in Section 7 with computational image stabilisation based on optical flow and online optimisation. We obtain real-time performance.

Before this we introduce notation and, in Section 2, our general approach to convergence proofs.

NOTATION

We write $x^{n:m} := (x^n, \dots, x^m)$ with $n \leq m$, and $x^{n:\infty} := (x^n, x^{n+1}, \dots)$. We also slice a set $\mathcal{B} \subset \prod_{k=0}^{\infty} X_k$ as $\mathcal{B}_{n:m} := \{x^{n:m} \mid x^{0:\infty} \in \mathcal{B}\}$ and $\mathcal{B}_n := \mathcal{B}_{n:n}$. We write $\mathbb{L}(X; Y)$ for the set of bounded linear operators between (Hilbert) spaces X and Y . We write $\text{Id} \in \mathbb{L}(X; X)$ for the identity operator. To not abuse norm notation for $M \in \mathbb{L}(X; X)$ that may not be positive semidefinite or self-adjoint, we set

$$\|x\|_M^2 := \langle x, x \rangle_M := \langle Mx, x \rangle.$$

We write $M \geq 0$ if M is positive semidefinite and $M \simeq N$ if $\| \cdot \|_M^2 = \| \cdot \|_N^2$.

For any set $A \subset X$ and $x \in X$ we write $\langle A, x \rangle := \{\langle z, x \rangle \mid z \in A\}$. We write δ_A for the $\{0, \infty\}$ -valued indicator function of A . For any $B \subset \mathbb{R}$ (in particular $B = \langle A, x \rangle$), we use the notation $B \geq 0$ to mean that $t \geq 0$ for all $t \in B$.

For $F : X \rightarrow (-\infty, \infty]$, we write $\text{dom } F := \{x \in X \mid F(x) < \infty\}$ for the effective domain. We call $F : X \rightarrow \overline{\mathbb{R}}$ *proper* if $F > -\infty$ and $\text{dom } F \neq \emptyset$. Let then F be convex. We write $\partial F(x)$ for the subdifferential at x and

$$\text{prox}_F(x) := \arg \min_{\tilde{x} \in X} F(x) + \frac{1}{2} \|\tilde{x} - x\|^2 = (\text{Id} + \partial F)^{-1}(x).$$

for the proximal map. We recall that F is strongly subdifferentiable at x with the factor $\gamma > 0$ if

$$F(\tilde{x}) - F(x) \geq \langle z, \tilde{x} - x \rangle + \frac{\gamma}{2} \|\tilde{x} - x\|^2 \quad \text{for all } z \in \partial F(x) \text{ and } \tilde{x} \in X.$$

In Hilbert spaces this is equivalent to strong convexity with the same factor [14].

Finally, for $f \in L^q(\Omega; \mathbb{R}^n)$, we write $\|f\|_{p,q} := \|\xi \mapsto \|f(\xi)\|_p\|_{L^q(\Omega)}$.

2 GENERAL PROXIMAL-TYPE ONLINE METHODS

We work towards the online solution of (1.1) by primal-dual methods from general principles. Indeed, as observed in [20], the PDPS for $\min[F + G \circ K]$ is simply a *preconditioned proximal point method* for a set-valued operator H whose roots encode the first-order primal-dual optimality conditions; we will return to them in Sections 4 and 5.

For any $H : X \rightrightarrows X$ and a preconditioner $M \in \mathbb{L}(X; X)$, such a method solves x^{k+1} from

$$0 \in H(x^{k+1}) + M(x^{k+1} - x^k) \quad (k \geq 0).$$

To develop an online version of this general scheme, we assume for $k \geq 1$ to be given $H_k : X_k \rightrightarrows X_k$ and linear preconditioners $M_k \in \mathbb{L}(X_k; X_k)$. Then we define x^{k+1} implicitly through

$$(PP) \quad 0 \in H_{k+1}(x^{k+1}) + M_{k+1}(x^{k+1} - z^{k+1}) \quad (k \geq 0).$$

The “base point” $z^{k+1} \in X_{k+1}$ is arbitrary in this section, but will later be predicted from x^k .

We analyse (PP) following the testing approach introduced in [33]. Our minor generalisation here incorporates the varying spaces $X_{k+1} \neq X$, *base points* $z^{k+1} \neq x^k$, and *comparison points* $\bar{x}^k \neq \hat{x}$, needed for “going dynamic”. The idea is to take *testing operators* $Z_k \in \mathbb{L}(X_k; X_k)$ that encode the convergence (or regret) rates that we test for, and apply the *tests* $\langle \cdot, x^{k+1} - \bar{x}^{k+1} \rangle_{Z_{k+1}}$ to the inclusions (PP), ($k \in \mathbb{N}$). Then simple manipulations yield estimates where $Z_k M_k$ forms a local metric for the convergence. Presently, we also include into the metric a factor Γ_k of the strong monotonicity of H_k , modelled abstractly by (2.1) in the next lemma. It also models gap functionals with \mathcal{G}_k^H . The prediction bound (2.2) is a Lipschitz-type condition between the base point and comparison sequences. Ideally the prediction penalty $p_{k+1} = 0$.

This will become more concrete in Sections 3 and 5.

Lemma 2.1. *On Hilbert spaces X_k , let $H_k : X_k \rightrightarrows X_k$, ($k = 1, \dots, N$), and $M_k, Z_k, \Gamma_k \in \mathbb{L}(X_k; X_k)$ with $Z_k M_k$ self-adjoint, ($k = 0, \dots, N$). Suppose (PP) is solvable for $\{x^k \in X_k\}_{k=1}^N$ given $\{z^k \in X_k\}_{k=1}^N$. Let $\{\bar{x}^k \in X_k\}_{k=0}^N$ and $x^0 \in X_0$. If for some $\mathcal{G}_k^H \in \mathbb{R}$ the fundamental condition*

$$(2.1) \quad \langle H_k(x^k), x^k - \bar{x}^k \rangle_{Z_k} \geq \frac{1}{2} \|x^k - \bar{x}^k\|_{\Gamma_k}^2 - \frac{1}{2} \|x^k - z^k\|_{Z_k M_k}^2 + \mathcal{G}_k^H \quad (k = 1, \dots, N)$$

holds, and for some $p_{k+1} \in \mathbb{R}$, the prediction bound

$$(2.2) \quad \frac{1}{2} \|z^{k+1} - \bar{x}^{k+1}\|_{Z_{k+1} M_{k+1}}^2 \leq \frac{1}{2} \|x^k - \bar{x}^k\|_{Z_k M_k + \Gamma_k}^2 + p_{k+1} \quad (k = 0, \dots, N-1)$$

holds, then so does

$$(2.3) \quad \frac{1}{2} \|x^N - \bar{x}^N\|_{Z_N M_N + \Gamma_N}^2 + \sum_{k=0}^{N-1} (\mathcal{G}_{k+1}^H - p_{k+1}) \leq \frac{1}{2} \|x^0 - \bar{x}^0\|_{Z_0 M_0 + \Gamma_0}^2.$$

Proof of Lemma 2.1. Let $k \in \{1, \dots, N\}$. Inserting (PP) into (2.1), we obtain

$$(2.4) \quad -\langle x^k - z^k, x^k - \bar{x}^k \rangle_{Z_k M_k} \geq \frac{1}{2} \|x^k - \bar{x}^k\|_{\Gamma_k}^2 - \frac{1}{2} \|x^k - z^k\|_{Z_k M_k}^2 + \mathcal{G}_k^H.$$

We recall for general self-adjoint M the Pythagoras' identity or three-point formula

$$\langle x^k - z^k, x^k - \bar{x}^k \rangle_M = \frac{1}{2} \|x^k - z^k\|_M^2 - \frac{1}{2} \|z^k - \bar{x}^k\|_M^2 + \frac{1}{2} \|x^k - \bar{x}^k\|_M^2.$$

Algorithm 3.1 Predictive online forward-backward splitting (POFB)

Require: For all $k \in \mathbb{N}$, on Hilbert spaces X_k , a primal predictor $A_k : X_k \rightarrow X_{k+1}$ and convex, proper, lower semicontinuous $F_{k+1}, G_{k+1} : X_{k+1} \rightarrow \overline{\mathbb{R}}$ such that G_{k+1} has Lipschitz gradient. Step length parameters $\tau_{k+1} > 0$.

- 1: Pick an initial iterate $x^0 \in X_0$.
- 2: **for** $k \in \mathbb{N}$ **do**
- 3: $z^{k+1} := A_k(x^k)$ ▷ prediction
- 4: $x^{k+1} := \text{prox}_{\tau_{k+1}G_{k+1}}(z^{k+1} - \tau_{k+1}\nabla F_{k+1}(z^{k+1}))$ ▷ forward-backward step
- 5: **end for**

Hence with $M = Z_k M_k$ we transform (2.4) into

$$\frac{1}{2} \|z^k - \bar{x}^k\|_{Z_k M_k}^2 \geq \frac{1}{2} \|x^k - \bar{x}^k\|_{Z_k M_k + \Gamma_k}^2 + \mathcal{G}_k^H.$$

Using (2.2) here we obtain for $k = 0, \dots, N-1$,

$$\frac{1}{2} \|x^{k+1} - \bar{x}^{k+1}\|_{Z_{k+1} M_{k+1} + \Gamma_{k+1}}^2 + (\mathcal{G}_{k+1}^H - p_{k+1}) \leq \frac{1}{2} \|x^k - \bar{x}^k\|_{Z_k M_k + \Gamma_k}^2.$$

Summing over $k = 0, \dots, N-1$, this gives (2.3). □

3 PREDICTIVE ONLINE FORWARD-BACKWARD SPLITTING

We review predictive online forward-backward splitting (POFB) for (1.1) with $K_k = \text{Id}$. This is useful to explain Section 2, online methods in general, and to later interpret the dual comparison sequence of the primal-dual method that is our main objective. We recall that given a step length parameter $\tau > 0$, forward-backward splitting for $\min[F + G]$ iterates

$$x^{k+1} := \text{prox}_{\tau G}(x^k - \tau \nabla F(x^k)).$$

For each $k \geq 1$, we take $F_k, G_k : X_k \rightarrow \overline{\mathbb{R}}$ convex, proper, and lower semicontinuous on a Hilbert space X_k . We assume ∇F_k to be L_k -Lipschitz and write $\gamma_{F_k}, \gamma_{G_k} \geq 0$ for the factors of (strong) subdifferentiability of F_k and G_k . We let $\Gamma_k := \varphi_k \tau_k \gamma_k \text{Id}$, $Z_k := \varphi_k \text{Id}$ and $M_k := \text{Id}$ for some step length, testing, and acceleration parameters $\tau_k, \varphi_k, \gamma_k > 0$. We also presume to be given predictors $A_k : X_k \rightarrow X_{k+1}$. We then set

$$H_k(x) := \tau_k [\partial G_k(x) + \nabla F_k(z^k)], \quad J_k := F_k + G_k, \quad \text{and} \quad z^{k+1} := A_k(x^k).$$

With this the abstract algorithm (PP) expands as Algorithm 3.1. We also let $\mathcal{B} \subset \prod_{k=0}^{\infty} X_k$ be a bounded comparison set of potential true solutions, write $\bar{x}^{0:\infty}$ for its elements, and $\mathcal{B}_{n:m}$ for the set of $\bar{x}^{n:m}$. These could be generated by true temporal coupling operators $\bar{A}_k : X_k \rightarrow X_{k+1}$ as in (1.5). Generally $A_k \neq \bar{A}_k$ due to measurement errors in the former.

3.1 REGRET THEORY

We need to verify the conditions of Lemma 2.1. We start with the prediction bound, which we interpret as a Lipschitz-like condition:

Lemma 3.1. *Fix $k \in \mathbb{N}$. In the overall setting of the present section, the prediction bound (2.2) holds with $p_{k+1} = \varepsilon_{k+1} \varphi_{k+1}$ for all $\bar{x}^{0:\infty} \in \mathcal{B}$ if for some $\Lambda_k > 0$ and $\varepsilon_{k+1} \in \mathbb{R}$ we have*

$$(3.1) \quad \varphi_{k+1} \leq \varphi_k (1 + \gamma_k \tau_k) \Lambda_k^{-1}$$

and

$$(3.2) \quad \frac{1}{2} \|A_k(x^k) - \bar{x}^{k+1}\|^2 \leq \frac{\Lambda_k}{2} \|x^k - \bar{x}^k\|^2 + \varepsilon_{k+1} \quad (\bar{x}^{0:\infty} \in \mathcal{B}).$$

Proof. The prediction bound (2.2) expands

$$\frac{\varphi_{k+1}}{2} \|A_k(x^k) - \bar{x}^{k+1}\|^2 \leq \frac{\varphi_k(1 + \gamma_k \tau_k)}{2} \|x^k - \bar{x}^k\|^2 + p_{k+1}.$$

By (3.2), this holds with $p_{k+1} = \varepsilon_{k+1} \varphi_{k+1}$ when φ_{k+1} satisfies (3.1). \square

To verify the fundamental condition (2.1), we recall the following *smoothness three-point inequalities* found in, e.g., [33, Appendix B] and [14, Chapter 7].

Lemma 3.2. *Suppose $F : X \rightarrow \overline{\mathbb{R}}$ is convex, proper, and lower semicontinuous, and has L -Lipschitz gradient. Then*

$$(3.3) \quad \langle \nabla F(z), x - \bar{x} \rangle \geq F(x) - F(\bar{x}) - \frac{L}{2} \|x - z\|^2 \quad (\bar{x}, z, x \in X).$$

If F is, moreover, γ -strongly convex, then for any $\beta > 0$,

$$(3.4) \quad \langle \nabla F(z), x - \bar{x} \rangle \geq F(x) - F(\bar{x}) + \frac{\gamma - \beta L^2}{2} \|x - \bar{x}\|^2 - \frac{1}{2\beta} \|x - z\|^2 \quad (\bar{x}, z, x \in X).$$

Lemma 3.3. *Fix $k \in \mathbb{N}$. In the overall setting of the present section, for some $\zeta_k \in (0, 1]$, suppose*

$$(3.5) \quad 0 \leq \gamma_k := \begin{cases} \gamma_{G_k} + \gamma_{F_k} - \tau_k \zeta_k^{-1} L_k^2, & \gamma_{F_k} > 0, \\ \gamma_{G_k}, & \gamma_{F_k} = 0 \text{ in which case we require } \tau_k L_k \leq \zeta_k. \end{cases}$$

Then (2.1) holds for

$$\mathcal{G}_k^H := \varphi_k \tau_k [J_k(x^k) - J_k(\bar{x}^k)] + \frac{\varphi_k(1 - \zeta_k)}{2} \|x^k - z^k\|^2.$$

Proof. Inserting H_k, Γ_k, Z_k, M_k , and \mathcal{G}_k^H , (2.1) divided by $\varphi_k \tau_k$ reads

$$(3.6) \quad \langle \partial G_k(x^k) + \nabla F_k(z^k), x^k - \bar{x}^k \rangle \geq J_k(x^k) - J_k(\bar{x}^k) + \frac{\gamma_k}{2} \|x^k - \bar{x}^k\|^2 - \frac{\zeta_k}{2\tau_k} \|x^k - z^k\|^2.$$

If $\gamma_{F_k} = 0$, (3.3) in Lemma 3.2 with the (strong) subdifferentiability of G_k yield

$$\langle \partial G_k(x^k) + \nabla F_k(z^k), x^k - \bar{x}^k \rangle \geq J_k(x^k) - J_k(\bar{x}^k) + \frac{\gamma_{G_k}}{2} \|x^k - \bar{x}^k\|^2 - \frac{L_k}{2} \|x^k - z^k\|^2.$$

This gives (3.6), hence the claim, when $\tau_k L_k \leq \zeta_k$ as ensured by (3.5) when $\gamma_{F_k} = 0$.

If $\gamma_{F_k} > 0$, by (3.4) in Lemma 3.2 for $\beta = \zeta_k^{-1} \tau_k$ and the (strong) subdifferentiability of G_k ,

$$\begin{aligned} \langle \partial G_k(x^k) + \nabla F_k(z^k), x^k - \bar{x}^k \rangle &\geq J_k(x^k) - J_k(\bar{x}^k) \\ &\quad + \frac{\gamma_{G_k} + \gamma_{F_k} - \zeta_k^{-1} \tau_k L_k^2}{2} \|x^k - \bar{x}^k\|^2 - \frac{\zeta_k}{2\tau_k} \|x^k - z^k\|^2. \end{aligned}$$

This gives (3.6), hence the claim, by the case $\gamma_{F_k} > 0$ of (3.5). \square

We now have the tools to study regret:

Theorem 3.4. *In the overall setting of this section, suppose (3.1), (3.2), and (3.5) hold for all $k = 0, \dots, N-1$ with $\zeta_k \in (0, 1]$ and $x^{1:N}$ generated by Algorithm 3.1 for an $x^0 \in X_0$. Then*

$$(3.7) \quad \sup_{\bar{x}^{1:N} \in \mathcal{B}_{1:N}} \sum_{k=1}^N \varphi_k \tau_k [J_k(x^k) - J_k(\bar{x}^k)] + \sum_{k=0}^{N-1} \frac{1 - \zeta_{k+1}}{2} \|x^{k+1} - A_k(x^k)\|^2 \\ \leq \sup_{\bar{x}^0 \in \mathcal{B}_0} \frac{\varphi_1}{2} \|x^0 - \bar{x}^0\|^2 + \sum_{k=1}^N \varepsilon_k \varphi_k.$$

Proof. Lemmas 3.1, 2.1 and 3.3 prove (2.3) for $\bar{x}^{0:\infty} \in \mathcal{U}$ with $p_{k+1} = \varepsilon_{k+1} \varphi_{k+1}$ as well as $Z_k M_k = \varphi_k \text{Id}$ and $\Gamma_k = \varphi_k \tau_k \gamma_k \text{Id}$. With this it reads

$$\frac{\varphi_N(1 + \gamma_N \tau_N)}{2\Lambda_N} \|x^N - \bar{x}^N\|^2 + \sum_{k=0}^{N-1} (\mathcal{G}_{k+1}^H - \varepsilon_{k+1} \varphi_{k+1}) \leq \frac{\varphi_0}{2} \|x^0 - \bar{x}^0\|^2.$$

We insert \mathcal{G}_{k+1}^H from Lemma 3.3 and take the supremum over $\bar{x}^{0:N} \in \mathcal{B}_{0:N}$ to prove the claim. \square

The next result is similar to [18, Theorem 4] when the forward-backward iteration does not cause the regret to increase: $1 + \gamma_k \tau \geq \Lambda_k$. Often in the online optimisation literature, $\text{regret}_B(x^1, \dots, x^N) \leq C\sqrt{N}$. The growing regret bound can arise from violating this step length condition or from the penalties $\sum_{k=1}^N \varepsilon_k$ in the prediction bound (3.2). For our purposes, bounding the regret in terms of the initialisation and the prediction bounds is enough.

Corollary 3.5. *In the overall setting of this section, take $\tau_k \equiv \tau$ and $\zeta_k \in (0, 1]$ and suppose (3.2), (3.5), and $1 + \gamma_k \tau \geq \Lambda_k$ hold for all $k = 0, \dots, N-1$ with $x^{1:N}$ generated by Algorithm 3.1 for an initial $x^0 \in X$. Then*

$$\text{dynamic_regret}_{\mathcal{B}_{1:N}}(x^1, \dots, x^N) + \sum_{k=0}^{N-1} \frac{1 - \zeta_{k+1}}{2\tau} \|x^{k+1} - A_k(x^k)\|^2 \leq \sup_{\bar{x}^0 \in \mathcal{B}_0} \frac{\|x^0 - \bar{x}^0\|^2}{2\tau} + \sum_{k=1}^N \frac{\varepsilon_k}{\tau}.$$

Proof. We take $\varphi_k \equiv 1$ in Theorem 3.4. \square

Remark 3.6 (Weighted dynamic regret). Suppose $1 + \gamma_k \tau_k > \Lambda_k$. Then $\{\varphi_k\}_{k \in \mathbb{N}}$ can increase in (3.1). If $\inf_k \tau_k > 0$, then (3.7) places more importance on J_k for large k : we regret early iterates less than recent. If $\frac{1 + \gamma_k \tau_k}{\Lambda_k} \geq c > 1$ and $\varphi_k = c^k \varphi_0$, this growth in importance is exponential, comparable to linear convergence on static problems; cf. [33]. With $F_{k+1} \equiv 0$ it is even possible to take $\tau_k \rightarrow \infty$ and obtain superexponential growth (superlinear convergence).

If, on the other hand $1 + \gamma_k \tau_k < \Lambda_k$, then (3.1) forces $\{\varphi_k\}_{k \in \mathbb{N}}$ to be decreasing. We therefore regret bad early iterates more than the recent. In the context of static optimisation problems, we are in the region of non-convergence or at most slow sub- $O(1/N)$ rates.

4 PARTIAL GAP FUNCTIONALS

We start our development of a primal-dual method by deriving meaningful measures of regret. We cannot in general obtain estimates on conventional duality gaps or on iterates, so need to consider alternative criteria. Throughout this section $F : X \rightarrow \overline{\mathbb{R}}$ and $G : Y \rightarrow \overline{\mathbb{R}}$ are convex, proper, and lower semicontinuous, and $K \in \mathbb{L}(X; Y)$ on Hilbert spaces X and Y . We recall that the first-order primal-dual optimality conditions for

$$\min_{x \in X} F(x) + G(Kx) \quad \text{equiv.} \quad \min_{x \in X} \max_{y \in Y} F(x) + \langle Kx, y \rangle - G^*(y)$$

are

$$(4.1) \quad -K\hat{y} \in \partial F(\hat{x}) \quad \text{and} \quad K^*\hat{x} \in \partial G^*(\hat{y}).$$

We call such a pair (\hat{x}, \hat{y}) a *critical point*.

4.1 COMMON GAP FUNCTIONALS

Let $T(x, y) := F(x) + G^*(y)$. Then the Fenchel conjugate $T^*(x^*, y^*) = F^*(x) + G(y)$. By the Fenchel–Young inequality

$$(4.2) \quad T(x, y) + T^*(x^*, y^*) \geq \langle x^*, x \rangle + \langle y^*, y \rangle \quad (x, x^* \in X; y, y^* \in Y)$$

with equality exactly when $(x^*, y^*) \in \partial T(x, y)$, equivalently, $(x, y) \in \partial T^*(x^*, y^*)$. Taking $x^* = -K^*y$ and $y^* = Kx$, either inclusion represents (4.1). Moreover, by (4.2), the *duality gap*

$$\mathcal{G}(x, y) := [F(x) + G(Kx)] + [F^*(-K^*y) + G^*(y)] = T(x, y) + T^*(-K^*y, Kx) \geq 0,$$

and is zero if and only if (4.1) holds. Taking the infimum over x and y we therefore prove the Fenchel–Rockafellar theorem.

We can expand

$$\mathcal{G}(x, y) = \sup_{(\bar{x}, \bar{y}) \in X \times Y} (\mathcal{L}(x, \bar{y}) - \mathcal{L}(\bar{x}, y))$$

for the Lagrangian

$$\mathcal{L}(x, y) := F(x) + \langle Kx, y \rangle - G^*(y).$$

This leads to the *Lagrangian duality gap*

$$\mathcal{G}^{\mathcal{L}}(x, y; \bar{x}, \bar{y}) := \mathcal{L}(x, \bar{y}) - \mathcal{L}(\bar{x}, y).$$

It is non-negative if (\bar{x}, \bar{y}) is a critical point, but may be zero even if (x, y) is not.

Since the Lagrangian duality gap is a relatively weak measure of optimality, and the true duality gap may not converge (fast), we define for bounded $B \subset X \times Y$ the *partial duality gap*

$$\mathcal{G}_B(x, y) := \sup_{(\bar{x}, \bar{y}) \in B} [\mathcal{L}(x, \bar{y}) - \mathcal{L}(\bar{x}, y)].$$

This is non-negative if B contains a critical point and equals the true duality gap \mathcal{G} if $B = X \times Y$. The partial gap converges ergodically for the basic unaccelerated PDPS [11].

4.2 PARTIAL PRIMAL GAPS

If we are not interested in the dual variable, we can define the *partial primal gap*

$$(4.3) \quad \hat{\mathcal{G}}_B(x) := \sup_{(\bar{x}, \bar{y}) \in B} \inf_{y \in Y} \mathcal{G}^{\mathcal{L}}(x, y; \bar{x}, \bar{y}).$$

We now try to interpret it.

Lemma 4.1. *Let $F : X \rightarrow \overline{\mathbb{R}}$ and $G : Y \rightarrow \overline{\mathbb{R}}$ be convex, proper, and lower semicontinuous, and $K \in \mathbb{L}(X; Y)$. Pick $B \subset X \times Y$. Then*

$$(4.4) \quad \hat{\mathcal{G}}_B(x) = [F + \check{G} \circ K](x) - \inf_{(\bar{x}, \bar{y}) \in B} [F + G \circ K](\bar{x})$$

for

$$(4.5) \quad \check{G}(y') := \sup_{\bar{x} \in X, \bar{y} \in Y} (\langle y', \bar{y} \rangle - G^*(\bar{y}) - J_B(\bar{x}, \bar{y})) - J_B^*(0, 0) \quad \text{and}$$

$$J_B(\bar{x}, \bar{y}) := F(\bar{x}) + G(K\bar{x}) + \delta_B(\bar{x}, \bar{y}).$$

Proof. We have

$$\begin{aligned} \inf_{y \in Y} \mathcal{G}^{\mathcal{L}}(x, y; \bar{x}, \bar{y}) &= \mathcal{L}(x, \bar{y}) - \sup_{y \in Y} \mathcal{L}(\bar{x}, y) \\ &= F(x) + \langle Kx, \bar{y} \rangle - G^*(\bar{y}) - [F + G \circ K](\bar{x}). \end{aligned}$$

Thus

$$\begin{aligned} \hat{\mathcal{G}}_B(x) &= F(x) + \sup_{\bar{x} \in X, \bar{y} \in Y} (\langle Kx, \bar{y} \rangle - G^*(\bar{y}) - [F + G \circ K](\bar{x}) - \delta_B(\bar{x}, \bar{y})) \\ &= F(x) + \sup_{\bar{x} \in X, \bar{y} \in Y} (\langle Kx, \bar{y} \rangle - G^*(\bar{y}) - J_B(\bar{x}, \bar{y})) = F(x) + \check{G}(Kx) + J_B^*(0, 0). \end{aligned}$$

Since $J_B^*(0, 0) = -\inf_{(\bar{x}, \bar{y}) \in B} [F + G \circ K](\bar{x})$, this establishes the claim. \square

Remark 4.2. If $B = B_X \times Y$ for some $B_X \subset X$, then $J_B(x, y)$ does not depend on y so that we obtain $\check{G} = G$. Thus the partial primal gap reduces to the difference of function values

$$\hat{\mathcal{G}}_{B_X \times Y}(x) = [F + G \circ K](x) - \inf_{\bar{x} \in B_X} [F + G \circ K](\bar{x}).$$

This gives an indication towards its meaningfulness. More generally, we will use the partial primal gap as the basis for a *marginalised primal regret* that “fails to regret” what $F + \check{G} \circ K \leq F + G \circ K$ cannot measure.

In the applications of Section 7, $G(y^1, \dots, y^N) = \sum_{k=1}^N \alpha \|Dy^k\|_{\mathcal{M}}$, compare (1.3), and B is a primal-dual extension $\mathcal{U}_{1:N}$ of $\mathcal{B}_{1:N}$ from (1.5). The construction of \check{G} convolves the static total variation regulariser G with the temporally coupled objective $J_{\mathcal{U}_{1:N}}$. The effect is to produce a new dynamic regulariser, alternative to [22, 37, 26, 25, 12, 28, 36]. The following instructive proposition elucidates how this works in general. However, the convexity assumption on B is not satisfied by $\mathcal{U}_{1:N}$. We write $E \square \tilde{E}$ for the infimal convolution of $E, \tilde{E} : X \rightarrow \overline{\mathbb{R}}$.

Proposition 4.3. *Suppose B is closed, convex, and nonempty, and both G and J_B are coercive. Then*

$$\check{G}(y') = \inf_{\tilde{y} \in Y} (G(y' - \tilde{y}) + J_B^*(0, \tilde{y}) - J_B^*(0, 0)).$$

Proof. We recall that $(E \square \tilde{E})^* = E^* + \tilde{E}^*$ for proper $E, \tilde{E} : X \rightarrow \overline{\mathbb{R}}$ [3, Proposition 13.21]. The infimal convolution $E \square \tilde{E}$ is convex, proper, and lower semicontinuous when E and \tilde{E} also are, E is coercive, and \tilde{E} is bounded from below [3, Propositions 12.14]. Since then $(E \square \tilde{E})^{**} = E \square \tilde{E}$, we obtain $E \square \tilde{E} = (E^* + \tilde{E}^*)^*$.

By the convexity of B , $J_B = J_B^{**}$. The coercivity of J_B implies that J_B^* is bounded from below.¹ Since G is coercive, taking $E(x, y) = G(y) + \delta_{\{0\}}(x)$ and $\tilde{E} = J_B^*$, we get

$$\begin{aligned} \check{G}(y') &= \sup_{\bar{x} \in X, \bar{y} \in Y} (\langle y', \bar{y} \rangle - G^*(\bar{y}) - J_B^*(\bar{x}, \bar{y})) - J_B^*(0, 0) \\ &= ([(\bar{x}, \bar{y}) \mapsto G^*(\bar{y})]^* \square J_B^*)(0, y') - J_B^*(0, 0) \\ &= ([(\bar{x}, \bar{y}) \mapsto G(\bar{y}) + \delta_{\{0\}}(\bar{x})] \square J_B^*)(0, y') - J_B^*(0, 0) \\ &= \inf_{\tilde{y} \in Y} (G(y' - \tilde{y}) + J_B^*(0, \tilde{y}) - J_B^*(0, 0)). \quad \square \end{aligned}$$

More generally, we can construct an infimal convolution lower bound with respect to the set of primal-dual minimisers of J_B . The coercivity assumption in the next lemma is fulfilled for F the squared distance or B bounded, both of which will be the case for the optical flow example.

¹Any coercive, convex, proper, lower semicontinuous function $E : X \rightarrow \overline{\mathbb{R}}$ has a minimiser \hat{x} . By the Fermat principle $0 \in \partial E(\hat{x})$. Thus $\hat{x} \in \partial E^*(0)$, which says exactly that $E^* \geq E^*(0)$.

Proposition 4.4. *Let $F : X \rightarrow \overline{\mathbb{R}}$ and $G : Y \rightarrow \overline{\mathbb{R}}$ be convex, proper, and lower semicontinuous, and $K \in \mathbb{L}(X; Y)$. Pick a closed subset $B \subset X \times Y$ and suppose J_B constructed from these components is coercive. Let*

$$\hat{B} := \{(\bar{x}, \bar{y}) \in B \mid J_B(\bar{x}, \bar{y}) = \inf J_B\} \quad \text{and} \quad \hat{B}_Y := \{\hat{y} \mid (\hat{x}, \hat{y}) \in \hat{B}\}.$$

Then \check{G} defined in (4.5) satisfies $\check{G} \geq (G^* + \delta_{\hat{B}_Y})^*$.

Proof. Since J_B is coercive, lower semicontinuous, and bounded from below, \hat{B} is non-empty. Since $\inf J_B = -J_B^*(0, 0)$, we calculate

$$\begin{aligned} \check{G}(y') &\geq \sup_{(\hat{x}, \hat{y}) \in \hat{B}} (\langle y', \hat{y} \rangle - G^*(\hat{y}) - J_B(\hat{x}, \hat{y})) - J_B^*(0, 0) \\ &= \sup_{\hat{y} \in \hat{B}_Y} (\langle y', \hat{y} \rangle - G^*(\hat{y})) = (G^* + \delta_{\hat{B}_Y})^*(y'). \quad \square \end{aligned}$$

Remark 4.5. If \hat{B}_Y is convex, then $\delta_{\hat{B}_Y} = \sigma_{\hat{B}_Y}^*$ for the support function $\sigma_{\hat{B}_Y}$. As this is convex, and lower semicontinuous, we get that $\check{G} \geq G \square \sigma_{\hat{B}_Y}$.

We always have $\check{G} \leq G$ since $-J_B^*(0, 0) \leq J_B(\bar{x}, \bar{y})$. The following establishes a lower bound on \check{G} in the our typical case of interest, with G a seminorm. It does not help interpret \check{G} , but will be sufficient for the application of the asymptotic theory in Section 6.

Lemma 4.6. *Let $F : X \rightarrow \overline{\mathbb{R}}$ be convex, proper, and lower semicontinuous, and let $G = \delta_{B_Y}^*$ be the support function of a closed convex set $B_Y \subset Y$. Pick $B \subset X \times B_Y$. Then \check{G} as defined in (4.5) satisfies $\check{G} \geq -G(-\cdot)$.*

Proof. $(\bar{x}, \bar{y}) \in \text{dom } J$ implies $\bar{y} \in B_Y$, hence $G^*(\bar{y}) = \delta_{B_Y}(\bar{y}) = 0$. Thus

$$\begin{aligned} \check{G}(y') &= \sup_{\bar{x} \in X, \bar{y} \in Y} (\langle y', \bar{y} \rangle - J_B(\bar{x}, \bar{y})) - J_B^*(0, 0) \\ &\geq \inf_{(\bar{x}, \bar{y}) \in B} \langle y', \bar{y} \rangle + \sup_{\bar{x} \in X, \bar{y} \in Y} (-J_B(\bar{x}, \bar{y})) - J_B^*(0, 0) \\ &\geq \inf_{\bar{y} \in B_Y} \langle y', \bar{y} \rangle = -\delta_{B_Y}^*(-y') = -G(-y'). \quad \square \end{aligned}$$

5 PREDICTIVE ONLINE PRIMAL-DUAL PROXIMAL SPLITTING

We now develop a predictive online version of the primal-dual proximal splitting (PDPS) of [11]. We assume for all $k \geq 1$ that $F_k : X_k \rightarrow \overline{\mathbb{R}}$ and $G_k^* : Y_k \rightarrow \overline{\mathbb{R}}$ are convex, proper, and lower semicontinuous, and $K_k \in \mathbb{L}(X_k; Y_k)$ on Hilbert spaces X_k and Y_k . With the general notation $u = (x, y)$, $u^k = (x^k, y^k)$, etc., for some step length parameters $\tau_k, \sigma_k > 0$, we set

$$(5.1) \quad H_k(u) := \begin{pmatrix} \partial F_k(x) + K_k^* y \\ \partial G_k^*(y) - K_k x \end{pmatrix} \quad \text{and} \quad M_k := \begin{pmatrix} \tau_k^{-1} \text{Id} & -K_k^* \\ -K_k & \sigma_k^{-1} \text{Id} \end{pmatrix}.$$

Then $0 \in H_k(\hat{u}^k)$ encodes the optimality conditions for the static problem (1.6) while $M_k \in \mathbb{L}(X_k \times Y_k; X_k \times Y_k)$ is the linear preconditioner for (PP).

We also take primal and dual predictors $A_k : X_k \rightarrow X_{k+1}$ and $B_k : Y_k \rightarrow Y_{k+1}$ and set

$$(5.2) \quad z^{k+1} = (\xi^{k+1}, v^{k+1}) := S_k(u^k), \quad S_k(u) := \begin{pmatrix} A_k(x) \\ \text{prox}_{\tilde{\sigma}_{k+1} \tilde{G}_{k+1}^*} (B_k(y) + \tilde{\sigma}_{k+1} K_{k+1} A_k(x)) \end{pmatrix},$$

forming the dual prediction v^{k+1} by taking an additional proximal step with respect to some $\tilde{\sigma}_{k+1} > 0$ and some $\tilde{\rho}_{k+1}$ -strongly convex, proper, and lower semicontinuous $\tilde{G}_{k+1}^* : Y_{k+1} \rightarrow \overline{\mathbb{R}}$. This is for proof-technical reasons.

Algorithm 5.1 Predictive online primal-dual proximal splitting (POPD)

Require: For all $k \in \mathbb{N}$, on Hilbert spaces X_k and Y_k , convex, proper, lower semicontinuous $F_{k+1} : X_{k+1} \rightarrow \overline{\mathbb{R}}$ and $G_{k+1}^*, \tilde{G}_{k+1}^* : Y_{k+1} \rightarrow \overline{\mathbb{R}}$, predictors $A_k : X_k \rightarrow X_{k+1}$ and $B_k : Y_k \rightarrow Y_{k+1}$, and $K_{k+1} \in \mathbb{L}(X_{k+1}; Y_{k+1})$. Step length parameters $\tau_{k+1}, \sigma_{k+1}, \tilde{\sigma}_{k+1} > 0$.

- 1: Pick initial iterates $x^0 \in X_0$ and $y^0 \in Y_0$.
- 2: **for** $k \in \mathbb{N}$ **do**
- 3: $\xi^{k+1} := A_k(x^k)$ ▷ primal prediction
- 4: $v^{k+1} := \text{prox}_{\tilde{\sigma}_{k+1}\tilde{G}_{k+1}^*}(B_k(y^k) + \tilde{\sigma}_{k+1}K_{k+1}\xi^{k+1})$ ▷ dual prediction
- 5: $x^{k+1} := \text{prox}_{\tau_{k+1}F_{k+1}}(\xi^{k+1} - \tau_{k+1}K_{k+1}^*v^{k+1})$ ▷ primal step
- 6: $y^{k+1} := \text{prox}_{\sigma_{k+1}G_{k+1}^*}(v^{k+1} + \sigma_{k+1}K_{k+1}(2x^{k+1} - \xi^{k+1}))$ ▷ dual step
- 7: **end for**

Example 5.1. We can always take, and in practise take, $\tilde{G}_{k+1}^* = G_{k+1}^* + \frac{\tilde{\rho}_{k+1}}{2} \|\cdot\|_{Y_{k+1}}^2$.

For the set of comparison sequences we take a bounded

$$(5.3a) \quad \mathcal{U} \subset \left\{ \bar{u}^{0:\infty} \in \prod_{k=0}^{\infty} X_k \times Y_k \mid \begin{array}{l} \bar{y}^{k+1} = \text{prox}_{\tilde{\sigma}_{k+1}\tilde{G}_{k+1}^*}(\bar{y}^{k+1} + \tilde{\sigma}_{k+1}K_{k+1}\bar{x}^{k+1}), \\ \text{for some } \tilde{y}^{k+1} =: \tilde{y}^{k+1}(\bar{u}^{k+1}) \in Y_{k+1}, \forall k \geq 0 \end{array} \right\}$$

and write

$$(5.3b) \quad \mathcal{B} := \{\bar{x}^{0:\infty} \mid \bar{u}^{0:\infty} \in \mathcal{U}\}.$$

As in (1.5), we could take $\bar{x}^{k+1} = \bar{A}_k(\bar{x}^k)$ and $\bar{y}^{k+1} = \bar{B}_k(\bar{y}^k)$ for some true temporal coupling operators $\bar{A}_k : X_k \rightarrow X_{k+1}$ and $\bar{B}_k : Y_k \rightarrow Y_{k+1}$.

We now derive regret estimates based on Lemma 2.1 and the partial primal gaps of Section 4. This revolves around verifying the assumptions of Lemma 2.1. Writing $\gamma_k, \rho_k \geq 0$ for the factors of (strong) convexity of F_k and G_k^* , respectively, for some $\eta_k > 0$ we take

$$(5.4) \quad Z_k := \eta_k \text{Id} \quad \text{and} \quad \Gamma_k = \eta_k \begin{pmatrix} \gamma_k \text{Id} & 2K_k^* \\ -2K_k & \rho_k \text{Id} \end{pmatrix}.$$

5.1 THE PREDICTION BOUND AND STEP LENGTH CONDITIONS

We need the following *strong non-expansivity* from the dual predictor:

Lemma 5.2. *On a Hilbert space X , suppose $F : X \rightarrow \overline{\mathbb{R}}$ is convex, proper, and γ -strongly subdifferentiable. Then prox_F is $(1 + \gamma)$ -strongly non-expansive:*

$$(1 + \gamma) \|\text{prox}_F(x) - \text{prox}_F(\tilde{x})\|_X \leq \langle \text{prox}_F(x) - \text{prox}_F(\tilde{x}), x - \tilde{x} \rangle \quad (x, \tilde{x} \in X).$$

Proof. Let $y := \text{prox}_F(x)$. By definition, for some $q \in \partial F(y)$ and $\tilde{q} \in \partial F(\tilde{y})$ we have $y + q = x$ and $\tilde{y} + \tilde{q} = \tilde{x}$. Since ∂F is γ -strongly monotone, $\langle q - \tilde{q}, y - \tilde{y} \rangle \geq \gamma \|y - \tilde{y}\|^2$. Thus

$$(1 + \gamma) \|y - \tilde{y}\|^2 = \langle y - \tilde{y}, x - \tilde{x} - (q - \tilde{q}) \rangle + \gamma \|y - \tilde{y}\|^2 \leq \langle y - \tilde{y}, x - \tilde{x} \rangle. \quad \square$$

We can now derive basic step length conditions.

Lemma 5.3. *In the overall setting of this section, fix $k \in \mathbb{N}$ and assume for some factors $\Lambda_k, \Theta_k > 0$ and prediction penalties $\varepsilon_{k+1}, \tilde{\varepsilon}_{k+1} \in \mathbb{R}$ the primal and dual prediction bounds*

$$(5.5a) \quad \frac{1}{2} \|A_k(x^k) - \bar{x}^{k+1}\|_{X_{k+1}}^2 \leq \frac{\Lambda_k}{2} \|x^k - \bar{x}^k\|_{X_k}^2 + \varepsilon_{k+1} \quad \text{and}$$

$$(5.5b) \quad \frac{1}{2} \|B_k(y^k) - \tilde{y}^{k+1}(\bar{u}^{k+1})\|_{Y_{k+1}}^2 \leq \frac{\Theta_k}{2} \|y^k - \tilde{y}^k\|_{Y_k}^2 + \tilde{\varepsilon}_{k+1} \quad (\bar{u}^{0:\infty} \in \mathcal{U}),$$

where \mathcal{U} and $\tilde{y}^{k+1}(\bar{u}^{k+1})$ are defined in (5.3a). Also assume for some $\kappa \in (0, 1)$ and testing parameters $\varphi_k, \psi_k > 0$, the step length conditions

$$(5.6a) \quad \eta_k = \varphi_k \tau_k = \psi_k \sigma_k,$$

$$(5.6b) \quad \tilde{\rho}_{k+1} \geq \frac{\Theta_k \eta_{k+1} \tilde{\sigma}_{k+1}^{-2}}{2\kappa(1 + \sigma_k \rho_k) \psi_k} + \frac{1}{2\sigma_{k+1}} - \tilde{\sigma}_{k+1}^{-1},$$

$$(5.6c) \quad \varphi_k(1 + \gamma_k \tau_k) \geq \varphi_{k+1} \Lambda_k + \frac{\varphi_k \tau_k \sigma_k \|K_k\|^2}{(1 - \kappa)(1 + \sigma_k \rho_k)}, \quad \text{and}$$

$$(5.6d) \quad 1 \geq \tau_k \sigma_k \|K_k\|^2$$

Then $Z_k M_k$ is self-adjoint and positive semidefinite, $Z_k M_k + \Gamma_k$ is positive semidefinite, and the prediction bound (2.2) holds with

$$(5.7) \quad p_{k+1} = \varphi_{k+1} \varepsilon_{k+1} + \frac{\kappa(1 + \sigma_k \rho_k) \psi_k}{2\Theta_k} \tilde{\varepsilon}_{k+1}.$$

The ‘‘testing’’ parameters $\varphi_k, \psi_k > 0$ model primal and dual convergence (or regret) rates. These are coupled by (5.6a) to the step length parameters. The condition (5.6b) restricts the parameters of the additional proximal step in the dual predictor while (5.6c) sets bounds on the step length parameters based on the available strong convexity and the Lipschitz-like factors of the predictors A_k and B_k . Finally, (5.6d) ensures that $Z_k M_k \geq 0$.

Proof. Using (5.6a) and Young’s inequality, we expand and estimate

$$(5.8) \quad Z_k M_k = \begin{pmatrix} \varphi_k \text{Id} & -\eta_k K_k^* \\ -\eta_k K_k & \psi_k \text{Id} \end{pmatrix} \geq \begin{pmatrix} \varphi_k \text{Id} - \eta_k^2 \psi_k^{-1} K_k^* K_k & 0 \\ 0 & \psi_k \text{Id} \end{pmatrix}.$$

Thus $Z_k M_k$ is self-adjoint due to (5.6a) and positive semidefinite due to (5.6d) and (5.6a). It follows, using Young’s inequality, that

$$(5.9) \quad Z_k M_k + \Gamma_k \simeq \begin{pmatrix} \varphi_k(1 + \gamma_k \tau_k) \text{Id} & -\eta_k K_k^* \\ -\eta_k K_k & \psi_k(1 + \rho_k \sigma_k) \text{Id} \end{pmatrix} \geq \begin{pmatrix} \varphi_k(1 + \gamma_k \tau_k) \text{Id} - \frac{\eta_k^2}{\psi_k(1 + \rho_k \sigma_k)} K_k^* K_k & 0 \\ 0 & \psi_k(1 + \rho_k \sigma_k) \text{Id} \end{pmatrix}.$$

Thus $Z_k M_k + \Gamma_k$ is positive semidefinite by (5.6c) and (5.6a).

We still need to prove (2.2). Writing $(\xi^{k+1}, v^{k+1}) := z^{k+1} = S_k(u^k)$, we have

$$(5.10) \quad \frac{1}{2} \|z^{k+1} - \bar{u}^{k+1}\|_{Z_{k+1} M_{k+1}}^2 = \frac{\varphi_{k+1}}{2} \|A_k(x^k) - \bar{x}^{k+1}\|^2 + \frac{\psi_{k+1}}{2} \|v^{k+1} - \bar{y}^{k+1}\|^2 - \eta_{k+1} \langle K_{k+1}(\xi^{k+1} - \bar{x}^{k+1}), v^{k+1} - \bar{y}^{k+1} \rangle$$

as well as

$$(5.11) \quad \frac{1}{2} \|u^k - \bar{u}^k\|_{Z_k M_k + \Gamma_k}^2 = \frac{\varphi_k(1 + \gamma_k \tau_k)}{2} \|x^k - \bar{x}^k\|^2 + \frac{\psi_k(1 + \rho_k \sigma_k)}{2} \|y^k - \bar{y}^k\|^2 - \eta_k \langle K_k(x^k - \bar{x}^k), y^k - \bar{y}^k \rangle.$$

Since \tilde{G}_{k+1} is $(\tilde{\rho}_{k+1}$ -strongly) convex, by Lemma 5.2, (5.2), and (5.3),

$$(1 + \tilde{\sigma}_{k+1} \tilde{\rho}_{k+1}) \|v^{k+1} - \bar{y}^{k+1}\|^2 \leq \langle v^{k+1} - \bar{y}^{k+1}, B_k(y^k) - \bar{y}^{k+1} + \tilde{\sigma}_{k+1} K_{k+1}(\xi^{k+1} - \bar{x}^{k+1}) \rangle.$$

By (5.6a) and (5.6b),

$$-\eta_{k+1}\tilde{\sigma}_{k+1}^{-1}(1 + \tilde{\sigma}_{k+1}\tilde{\rho}_{k+1}) + \frac{\Theta_k\eta_{k+1}^2\tilde{\sigma}_{k+1}^{-2}}{2\kappa(1 + \sigma_k\rho_k)\psi_k} \leq -\frac{\psi_{k+1}}{2}.$$

Consequently, also using (5.6a), (5.5b), and Young's inequality, we obtain

$$\begin{aligned} & -\eta_{k+1}\langle K_{k+1}(\xi^{k+1} - \bar{x}^{k+1}), v^{k+1} - \bar{y}^{k+1} \rangle \\ &= -\eta_{k+1}\tilde{\sigma}_{k+1}^{-1}\langle B_k(y^k) - \bar{y}^{k+1} + \tilde{\sigma}_{k+1}K_{k+1}(\xi^{k+1} - \bar{x}^{k+1}), v^{k+1} - \bar{y}^{k+1} \rangle \\ &\quad + \eta_{k+1}\tilde{\sigma}_{k+1}^{-1}\langle B_k(y^k) - \bar{y}^{k+1}, v^{k+1} - \bar{y}^{k+1} \rangle \\ &\leq -\eta_{k+1}\tilde{\sigma}_{k+1}^{-1}(1 + \tilde{\sigma}_{k+1}\tilde{\rho}_{k+1})\|v^{k+1} - \bar{y}^{k+1}\|^2 + \eta_{k+1}\tilde{\sigma}_{k+1}^{-1}\langle B_k(y^k) - \bar{y}^{k+1}, v^{k+1} - \bar{y}^{k+1} \rangle \\ &\leq -\frac{\psi_{k+1}}{2}\|v^{k+1} - \bar{y}^{k+1}\|^2 + \frac{\kappa(1 + \sigma_k\rho_k)\psi_k}{2\Theta_k}\|B_k(y^k) - \bar{y}^{k+1}\|^2. \\ &\leq -\frac{\psi_{k+1}}{2}\|v^{k+1} - \bar{y}^{k+1}\|^2 + \frac{\kappa(1 + \sigma_k\rho_k)\psi_k}{2\Theta_k}\left(\frac{\Theta_k}{2}\|y^k - \bar{y}^k\|^2 + \tilde{\varepsilon}_{k+1}\right). \end{aligned}$$

Applying this and (5.5a) in (5.10), and observing the definition of p_{k+1} in (5.7), we obtain

$$(5.12) \quad \frac{1}{2}\|z^{k+1} - \bar{u}^{k+1}\|_{Z_{k+1}M_{k+1}}^2 \leq \frac{\varphi_{k+1}\Lambda_k}{2}\|x^k - \bar{x}^k\|^2 + \frac{\kappa(1 + \sigma_k\rho_k)\psi_k}{2}\|y^k - \bar{y}^k\|^2 + p_{k+1}.$$

We also have by Young's inequality

$$\begin{aligned} & \eta_k\langle K_k(x^k - \bar{x}^k), y^k - \bar{y}^k \rangle \\ &\leq \frac{\eta_k^2}{2(1 - \kappa)(1 + \sigma_k\rho_k)\psi_k}\|K_k(x^k - \bar{x}^k)\|^2 + \frac{(1 - \kappa)(1 + \sigma_k\rho_k)\psi_k}{2}\|y^k - \bar{y}^k\|^2. \end{aligned}$$

Hence (5.11) gives

$$(5.13) \quad -\frac{1}{2}\|u^k - \bar{u}^k\|_{Z_kM_k+\Gamma_k}^2 \leq \left(\frac{\eta_k^2\|K_k\|^2}{2(1 - \kappa)(1 + \sigma_k\rho_k)\psi_k} - \frac{\varphi_k(1 + \gamma_k\tau_k)}{2}\right)\|x^k - \bar{x}^k\|^2 - \frac{\kappa(1 + \sigma_k\rho_k)\psi_k}{2}\|y^k - \bar{y}^k\|^2.$$

Combined, (5.12) and (5.13) show that

$$\begin{aligned} & \frac{1}{2}\|z^{k+1} - \bar{u}^{k+1}\|_{Z_{k+1}M_{k+1}}^2 - \frac{1}{2}\|u^k - \bar{u}^k\|_{Z_kM_k+\Gamma_k}^2 \leq \varphi_{k+1}\varepsilon_{k+1} + p_{k+1} \\ &\quad + \left(\frac{\varphi_{k+1}\Lambda_k}{2} + \frac{\eta_k^2\|K_k\|^2}{2(1 - \kappa)(1 + \sigma_k\rho_k)\psi_k} - \frac{\varphi_k(1 + \gamma_k\tau_k)}{2}\right)\|x^k - \bar{x}^k\|^2. \end{aligned}$$

From here (5.6c) shows (2.2) with p_{k+1} given by (5.7). □

The proof of the next lemma is immediate:

Lemma 5.4. *The right hand side of (5.6b) is minimised by $\tilde{\sigma}_{k+1} = \frac{\Theta_k\eta_{k+1}}{\kappa(1 + \sigma_k\rho_k)\psi_k}$. With this choice (5.6b) reads $2\eta_{k+1}\tilde{\rho}_{k+1} \geq \psi_{k+1} - \kappa\Theta_k^{-1}(1 + \sigma_k\rho_k)\psi_k$.*

The following example, that employs Lemma 5.4, provides our practical step length rules.

Example 5.5 (Constant step length and testing parameters). For some $\tau, \sigma > 0$ and $\kappa \in (0, 1)$ take $\tau_k \equiv \tau$, $\sigma_k \equiv \sigma$, and $\tilde{\sigma}_{k+1} = \frac{\Theta_k \sigma}{\kappa(1+\sigma\rho_k)}$. Then (5.6) holds with $\eta_k \equiv \tau$, $\varphi_k \equiv 1$, and $\psi_k \equiv \frac{\tau}{\sigma}$ if

$$\tilde{\rho}_{k+1} \geq \frac{1}{2\sigma} \left(1 - \frac{\kappa(1+\sigma\rho_k)}{\Theta_k} \right), \quad 1 + \gamma_k \tau \geq \Lambda_k + \frac{\tau\sigma \|K_k\|^2}{(1-\kappa)(1+\sigma\rho_k)}, \quad \text{and} \quad 1 \geq \tau\sigma \|K_k\|^2.$$

In particular with $\rho_k = 0$, $\tilde{\rho}_{k+1} \equiv \tilde{\rho}$, $\gamma_k \equiv \gamma$, and $\Theta_k \equiv \Theta$, and $\Lambda_k \equiv \Lambda$, we have $\tilde{\sigma}_{k+1} \equiv \tilde{\sigma} = \frac{\Theta\sigma}{\kappa}$, and need

$$\tilde{\rho} \geq \frac{1-\kappa\Theta^{-1}}{2\sigma}, \quad 1 + \gamma\tau \geq \Lambda + \frac{\tau\sigma \|K_k\|^2}{1-\kappa}, \quad \text{and} \quad 1 \geq \tau\sigma \|K_k\|^2.$$

This gives no growth for the testing parameters φ_k and ψ_k , hence Lemma 2.1 can provide no simple convergence result. Indeed, looking at (2.3), to get iterate convergence, $Z_k M_k + \Gamma_k$ needs to grow as $k \rightarrow \infty$. This can be reduced to the growth of φ_k and ψ_{k+1} ; compare (5.9).

Example 5.6 (Exponential testing parameters with constant step lengths). For some $\tau, \sigma > 0$ and $\kappa \in (0, 1)$, take $\tau_k \equiv \tau$, $\sigma_{k+1} \equiv \sigma$, as well as $\tilde{\sigma}_{k+1} = \kappa^{-1}\Theta_k\sigma$. Then (5.6) holds with $\eta_k = \varphi_k\tau$, $\varphi_{k+1} = \varphi_k(1 + \rho_k\sigma)$, and $\psi_k = \frac{\tau}{\sigma}\varphi_k$ provided

$$\tilde{\rho}_{k+1} \geq \frac{1-\kappa\Theta_k^{-1}}{2\sigma}, \quad 1 + \gamma_k \tau \geq \frac{\tau\sigma \|K_k\|^2}{(1-\kappa)(1+\rho_k\sigma)} + (1+\rho_k\sigma)\Lambda_k, \quad \text{and} \quad 1 \geq \tau\sigma \|K_k\|^2.$$

However, due to (5.7), we cannot expect convergence unless the prediction penalties ε_{k+1} and $\tilde{\varepsilon}_{k+1}$ from (5.5) go fast to zero. This practically means that $\bar{x}^{k+1} = A_k(\bar{x}^k)$ and $\bar{y}^{k+1} = B_k(\bar{y}^k)$ with A_k and B_k non-expansive—not satisfied in our applications of interest. We therefore concentrate on the setting of Example 5.5, and attempt to get an acceptable form of regret out of (2.3). To do so, and to apply Lemma 2.1, we still need to verify (2.1) for a useful \mathcal{G}_k^H .

5.2 THE FUNDAMENTAL CONDITION AND GAP FUNCTIONALS

Lemma 5.7. *In the overall setting of the present section, (2.1) holds for*

$$\begin{aligned} \mathcal{G}_{k+1}^H &:= \eta_k [F_{k+1}(x^{k+1}) - F_{k+1}(\bar{x}^{k+1}) + G_{k+1}^*(y^{k+1}) - G_{k+1}^*(\bar{y}^{k+1}) \\ &\quad - \langle K_{k+1}^* y^{k+1}, \bar{x}^{k+1} \rangle + \langle K_{k+1} x^{k+1}, \bar{y}^{k+1} \rangle] + \frac{1}{2} \|u^{k+1} - S_k(u^k)\|_{Z_{k+1}M_{k+1}}^2. \end{aligned}$$

Proof. Insert H_k from (5.1) and Γ_k and Z_k from (5.4) with $z^{k+1} = S_k(u^k)$ into (2.1). \square

We need to further estimate and interpret \mathcal{G}_{k+1}^H . To do this, we let

$$\begin{aligned} F_{1:N}(x^{1:N}) &:= \sum_{k=0}^{N-1} \eta_k F_{k+1}(x^{k+1}), \quad G_{1:N}(y^{1:N}) := \sum_{k=0}^{N-1} \eta_k G_{k+1}(\eta_k^{-1} y^{k+1}), \quad \text{and} \\ K_{1:N} x^{1:N} &:= (\eta_0 K_1 x^1, \dots, \eta_{N-1} K_N x^N). \end{aligned}$$

Observe that $G_{1:N}^*(y^{1:N}) = \sum_{k=0}^{N-1} \eta_k G_{k+1}^*(y^{k+1})$. We recall the comparison sets \mathcal{U} and \mathcal{B} and from (5.3) and the slicing notation $\mathcal{U}_{n:m}$ and $\mathcal{B}_{n:m}$ from Section 1.

By Lemma 4.1 applied to $K = K_{1:N}$, $F = F_{1:N}$ and $G^* = G_{1:N}^*$ we obtain

$$(5.14) \quad \begin{aligned} \sup_{\bar{u}^{1:N} \in \mathcal{U}_{1:N}} \sum_{k=0}^{N-1} \mathcal{G}_{k+1}^H &\geq \sum_{k=0}^{N-1} \frac{1}{2} \|u^{k+1} - \bar{S}_k(u^k)\|_{Z_{k+1}M_{k+1}}^2 \\ &\quad + [F_{1:N} + \check{G}_{1:N} \circ K_{1:N}](x^{1:N}) - \inf_{\bar{x}^{1:N} \in \mathcal{B}_{1:N}} [F_{1:N} + G_{1:N} \circ K_{1:N}](\bar{x}^{1:N}) \end{aligned}$$

for

$$(5.15) \quad \check{G}_{1:N}(y'_{1:N}) = \sup_{\bar{x}^{1:N}, \bar{y}^{1:N}} \left(\langle y'_{1:N}, \bar{y}^{1:N} \rangle - G_{1:N}^*(\bar{y}^{1:N}) - J_{\mathcal{U}_{1:N}}(\bar{x}^{1:N}, \bar{y}^{1:N}) \right) - J_{\mathcal{U}_{1:N}}^*(0, 0)$$

with the supremum running over $\bar{x}^{1:N} \in X_1 \times \dots \times X_N$ and $\bar{y}^{1:N} \in Y_1 \times \dots \times Y_N$ and with

$$J_{\mathcal{U}_{1:N}}(\bar{x}^{1:N}, \bar{y}^{1:N}) := [F_{1:N} + G_{1:N} \circ K_{1:N}](\bar{x}^{1:N}) + \delta_{\mathcal{U}_{1:N}}(\bar{x}^{1:N}, \bar{y}^{1:N}).$$

Observe that

$$[F_{1:N} + G_{1:N} \circ K_{1:N}](x^{1:N}) = \sum_{k=0}^{N-1} \eta_k [F_{k+1} + G_{k+1} \circ K_{k+1}](x^{k+1}).$$

We are now ready for our main estimate. It says that subject to how well we can measure with $\check{G}_{1:N}$ in place of $G_{1:N}$, the *marginalised primal regret* of the primal iterates $x^{1:N}$ compared to the best $\bar{x}^{1:N} \in \mathcal{B}_{1:N}$ remains bounded by the initialisation and the prediction penalties.

Theorem 5.8. *In the overall setting of this section, suppose the prediction (5.5) and step length bounds (5.6) hold for $u^{1:N}$ generated by Algorithm 5.1 for an initial $u^0 \in X_0 \times Y_0$. Then*

$$\begin{aligned} & [F_{1:N} + \check{G}_{1:N} \circ K_{1:N}](x^{1:N}) - \inf_{\bar{x}^{1:N} \in \mathcal{B}_{1:N}} [F_{1:N} + G_{1:N} \circ K_{1:N}](\bar{x}^{1:N}) + \sum_{k=0}^{N-1} \frac{\|u^{k+1} - S_k(u^k)\|_{Z_{k+1}M_{k+1}}^2}{2} \\ & \leq e_N := \sup_{\bar{u}^0 \in \mathcal{U}_0} \frac{1}{2} \|\bar{u}^0 - u^0\|_{Z_0M_0 + \Gamma_0}^2 + \sum_{k=0}^{N-1} \left(\varepsilon_{k+1} \varphi_{k+1} + \frac{\kappa(1 + \sigma_k \rho_k) \psi_k}{2\Theta_k} \tilde{\varepsilon}_{k+1} \right). \end{aligned}$$

Proof. Lemmas 5.3 and 5.7 verify the conditions of Lemma 2.1 for $\bar{u}^{0:N} \in \mathcal{U}$ with p_{k+1} as in (5.7) and $Z_N M_N + \Gamma_N \geq 0$. Therefore, taking the supremum over $\bar{u}^{0:N} \in \mathcal{U}_{0:N}$ in (2.3), we get

$$\sup_{\bar{u}^{0:N} \in \mathcal{U}_{0:N}} \sum_{k=0}^{N-1} \mathcal{G}_{k+1}^H \leq e_N.$$

Inserting (5.14) we obtain the claim. \square

Remark 5.9 (Interpretation of the dual comparison sequence). Let $\bar{y}^{k+1} = \bar{B}_k(\bar{y}^k)$ for a dual temporal coupling operator \bar{B}_k . Then (5.3) updates the dual comparison variable as

$$(5.16) \quad \bar{y}^{k+1} := \text{prox}_{\tilde{\sigma}_{k+1} \tilde{G}_{k+1}^*}(\bar{B}_k(\bar{y}^k) + \tilde{\sigma}_{k+1} \bar{x}^{k+1})$$

This amounts to the POFB of Section 3 applied with the predictor \bar{B}_k and the step length parameter $\tau_{k+1} = \tilde{\sigma}_{k+1}$ to the formal problem

$$\min_{y^1, y^2, \dots} \sum_{k=1}^{\infty} \tilde{G}_k^*(y^k) - \langle K_k \bar{x}^k, y^k \rangle, \quad y^{k+1} = \bar{B}_k(y^k)$$

An “optimal” \hat{y}^k , achieving $\inf_y \tilde{G}_k^*(y) - \langle K_k \bar{x}^k, y \rangle$, would give

$$[F_k + \tilde{G}_k \circ K_k](\bar{x}^k) = F_k(\bar{x}^k) + \langle K_k \bar{x}^k, \hat{y}^k \rangle - \tilde{G}_k^*(\hat{y}^k).$$

This is approximated by \bar{y}^{k+1} generated by (5.16), better as $\tilde{\sigma}_k \rightarrow \infty$. In the setting of Example 5.1, if we can also let $\tilde{\rho}_k \rightarrow \rho_k$, then we get closer to calculating $[F_k + G_k \circ K_k](\bar{x}^k)$.

6 REGULARISATION THEORY

We now study online optimisation methods as regularisation methods for dynamic inverse problems. More precisely, we study asymptotic behaviour as the corruption of the data vanishes. *We will not, in the confines of this paper, attempt to produce convergence rates or convergence to minimum-norm solutions, as is commonly done [15].* For the denoising-based optical flow problem the latter is not even necessary. Similar optimisation-based ideas that we present have been presented for non-linear static inverse problems in [24].

6.1 GENERAL RESULTS

Our basic setup is the following. For each corruption (noise) level $\delta > 0$ of the data and time index $N \in \mathbb{N}$, we are given a function $J_N^\delta : X_N \rightarrow \overline{\mathbb{R}}$ that we would ideally like to minimise. We know that in the limit as $\delta \searrow 0$, the ground-truth is in a set $B_N \subset X_N$. In practise we only know inexact minimisers x_δ^N of J_N^δ , or not even that: we can only measure the fit through \tilde{J}_N^δ . More precisely we know that the values of regret functional

$$(6.1) \quad R_N^\delta(x) := \sup_{\bar{x}^N \in B_N} \left(\tilde{J}_N^\delta(x) - J_N^\delta(\bar{x}^N) \right)$$

go asymptotically below zero. Based on this information, we would like x_δ^N to convergence to a ground-truth as both $N \rightarrow \infty$ and $\delta \searrow 0$. In the present subsection, under additional technical conditions, we show that the function values $\tilde{J}_N^\delta(x_\delta^N)$ asymptotically agree with $\inf_{B_N} J_N^\delta$. In the next subsection we apply this result to functionals with a more specific Tikhonov structure.

Lemma 6.1. *On sets X_N , let $J_N^\delta, \tilde{J}_N^\delta : X_N \rightarrow \overline{\mathbb{R}}$ be proper for $\delta \geq 0$ and $N \in \mathbb{N}$. For each $N \in \mathbb{N}$ let, moreover, $B_N \subset X_N$ be such that $B_N \cap \text{dom } J_N^0 \neq \emptyset$ and*

$$(6.2) \quad 0 \leq \liminf_{\delta \searrow 0, N \rightarrow \infty} \left(\inf_{X_N} \tilde{J}_N^\delta - \inf_{B_N} J_N^\delta \right).$$

For every $\delta > 0$, suppose there exists $N(\delta) \in \mathbb{N}$ and $x_\delta^N \in X_N$, ($N \in \mathbb{N}$), such that

$$(6.3) \quad \limsup_{\delta \searrow 0} \sup_{N \geq N(\delta)} R_N^\delta(x_\delta^N) \leq 0.$$

Then there exists $\bar{N}(\delta) \geq N(\delta)$ such that

$$(6.4) \quad \lim_{\delta \searrow 0} \sup_{N \geq \bar{N}(\delta)} R_N^\delta(x_\delta^N) = \lim_{\delta \searrow 0} \inf_{N \geq \bar{N}(\delta)} R_N^\delta(x_\delta^N) = 0.$$

Proof. Using (6.3), for any $\bar{N}(\delta) \geq N(\delta)$ we estimate

$$(6.5) \quad \begin{aligned} 0 &\geq \limsup_{\delta \searrow 0} \sup_{N \geq \bar{N}(\delta)} R_N^\delta(x_\delta^N) \geq \liminf_{\delta \searrow 0} \inf_{N \geq \bar{N}(\delta)} R_N^\delta(x_\delta^N) \\ &= \liminf_{\delta \searrow 0} \inf_{N \geq \bar{N}(\delta)} \left(\tilde{J}_N^\delta(x_\delta^N) - \inf_{B_N} J_N^\delta \right) \geq \liminf_{\delta \searrow 0} \inf_{N \geq \bar{N}(\delta)} \left(\inf_{X_N} \tilde{J}_N^\delta - \inf_{B_N} J_N^\delta \right). \end{aligned}$$

Taking $\bar{N}(\delta)$ large enough, (6.2) shows that the last term is non-negative. Consequently

$$\limsup_{\delta \searrow 0} \sup_{N \geq \bar{N}(\delta)} R_N^\delta(x_\delta^N) = \liminf_{\delta \searrow 0} \inf_{N \geq \bar{N}(\delta)} R_N^\delta(x_\delta^N) = 0.$$

Since both $\limsup \sup \geq \liminf \sup \geq \liminf \inf$ and $\limsup \sup \geq \limsup \inf \geq \liminf \inf$, the claim follows. \square

Lemma 6.2. *The condition (6.2) holds if*

$$(6.6) \quad \limsup_{\delta \rightarrow 0, N \rightarrow \infty} \inf_{B_N} J_N^\delta \leq \liminf_{\delta \rightarrow 0, N \rightarrow \infty} \inf_{X_N} \tilde{J}_N^\delta.$$

In this case, Lemma 6.1 implies

$$(6.7) \quad \lim_{\delta \rightarrow 0} \sup_{N \geq \bar{N}(\delta)} \tilde{J}_N^\delta(x_\delta^N) = \limsup_{\delta \rightarrow 0} \sup_{N \geq \bar{N}(\delta)} \inf_{B_N} J_N^\delta.$$

Proof. That (6.2) holds is clear. Using (6.4) and (6.6) we also have

$$0 = \liminf_{\delta \rightarrow 0} \inf_{N \geq \bar{N}(\delta)} \left(\tilde{J}_N^\delta(x_\delta^N) - \inf_{B_N} J_N^\delta \right) \geq \liminf_{\delta \rightarrow 0} \inf_{N \geq \bar{N}(\delta)} \tilde{J}_N^\delta(x_\delta^N) - \limsup_{\delta \rightarrow 0} \sup_{N \geq \bar{N}(\delta)} \inf_{B_N} J_N^\delta \geq 0.$$

Likewise $\limsup_{\delta \rightarrow 0} \sup_{N \geq \bar{N}(\delta)} \tilde{J}_N^\delta(x_\delta^N) = \limsup_{\delta \rightarrow 0} \sup_{N \geq \bar{N}(\delta)} \inf_{B_N} J_N^\delta$. Together these give the claim. \square

6.2 ONLINE METHODS AND PROBLEMS WITH TIKHONOV STRUCTURE

For Tikhonov-style regularisation and online methods, we collect assumptions in the following. For simplicity, we assume all the functions to be non-negative and only involve the data terms F_k^δ in \tilde{J}_N^δ .

Assumption 6.3 (Dynamic Tikhonov pairs). For all $k \geq 1$ and $\delta \geq 0$, on sets X_k , let $F_k^\delta, G_k^\delta : X_k \rightarrow [0, \infty]$. Define

$$J_N^\delta(x^{1:N}) := \frac{1}{N} \sum_{k=1}^N \left(F_k^\delta(x^k) + G_k^\delta(x^k) \right) \quad \text{and} \quad \tilde{J}_N^\delta(x^{1:N}) := \frac{1}{N} \sum_{k=1}^N F_k^\delta(x^k).$$

For some sets $\mathcal{B} \subset \prod_{k=1}^\infty X_k$ of *potential ground-truths*, we suppose both

$$(6.8a) \quad \limsup_{\delta \rightarrow 0, N \rightarrow \infty} \inf_{\bar{x}^{1:N} \in \mathcal{B}_{1:N}} \sum_{k=1}^N \frac{1}{N} F_k^\delta(\bar{x}^k) = 0$$

and

$$(6.8b) \quad \limsup_{\delta \rightarrow 0, N \rightarrow \infty} \sup_{\bar{x}^{1:N} \in \mathcal{B}_{1:N}} \sum_{k=1}^N \frac{1}{N} G_k^\delta(\bar{x}^k) = 0.$$

Since $F_k^\delta \geq 0$, (6.8a) says that $\mathcal{B}_{1:N}$ asymptotically approximates the ground-truth. For (6.8b) to hold, the regularisation has to asymptotically vanish for all potential ground-truths.

Note that in the context of [Assumption 6.3](#), the dynamic regret of (6.1) can be written

$$(6.9) \quad R_N^\delta(x^{1:N}) = \sup_{\bar{x}^{1:N} \in \mathcal{B}_{1:N}} \sum_{k=1}^N \frac{1}{N} \left(F_k^\delta(x^k) - F_k^\delta(\bar{x}^k) - G_k^\delta(\bar{x}^k) \right).$$

Example 6.4 (Squared data term). With each X_k a normed space, let $F_k^\delta(x) := \frac{1}{2} \|x - b_\delta^k\|^2$, where b_δ^k is a noisy version of \bar{b}^k . Then (6.8a) reduces to

$$\limsup_{\delta \rightarrow 0, N \rightarrow \infty} \inf_{\bar{x}^{1:N} \in \mathcal{B}_N} \sum_{k=1}^N \frac{1}{2N} \|\bar{x}^k - b_\delta^k\|^2 = 0.$$

If $\mathcal{B} \ni \bar{b}^{1:\infty}$ and the noise level $\|\bar{b}^k - b_\delta^k\|^2 \leq \delta$ for all k , then the condition (6.8a) holds.

Example 6.5 (Norm regularisation). Let $G_k^\delta(x) := \alpha(\delta)G(x)$ for a positively homogeneous and Lipschitz G on a normed space X , and a regularisation parameter $\alpha(\delta) \searrow 0$ as $\delta \searrow 0$. Then (6.8b) holds if $\mathcal{B} \subset B^\mathbb{N}$ with $B \subset X$ bounded. In particular G can be a semi-norm as in (1.3).

Theorem 6.6 (Dynamic Tikhonov-style regularisation). Let Assumption 6.3 hold and x_δ^N be an ε_δ^N -minimiser of J_N^δ with $\lim_{\delta \searrow 0, N \rightarrow \infty} \varepsilon_\delta^N = 0$. Then (6.4) holds for some $\bar{N}(\delta) \rightarrow \infty$ and

$$(6.10) \quad \lim_{\delta \searrow 0} \sup_{N \geq \bar{N}(\delta)} \sum_{k=1}^N \frac{1}{N} F_k^\delta(x^k) = 0.$$

Proof. (6.3) holds by $\varepsilon_\delta^N \searrow 0$, and (6.6) by (6.8) and $F_k^\delta \geq 0$. Lemmas 6.1 and 6.2 show (6.7) for some $\bar{N}(\delta)$. Assumption 6.3 gives $\limsup_{\delta \searrow 0} \sup_{N \geq \bar{N}(\delta)} \inf_{B_N} J_N^\delta = 0$, so (6.7) is (6.10). \square

Example 6.7 (Squared data term, continued). In the context of Example 6.4, (6.10) reads

$$\lim_{\delta \searrow 0} \sup_{N \geq \bar{N}(\delta)} \sum_{k=1}^N \frac{1}{2N} \|\bar{x}_\delta^k - b_\delta^k\|^2 = 0.$$

In other words, the iterates \bar{x}_δ^{k+1} asymptotically get closer to the data as δ goes down. Combined with $\|b_0^k - b_\delta^k\|^2 \leq \delta$ from Example 6.4, this readily shows them to converge to the ground-truth.

To apply these ideas to predictive online optimisation methods, the idea is to apply algorithms to $F_k = F_k^\delta$ and $G_k = G_k^\delta$ as well as some predictor A_k^δ (and B_k^δ) for fixed $\delta > 0$. The algorithms are parametrised independent of δ , although any factors of strong convexity, as well as the parameters from the prediction bounds (3.2) and (5.5) may depend on the corruption level δ . Without explicitly introducing as such, we indicate with appropriate superscript or subscript δ any variables from Sections 3 and 5 that now depend on δ .

Theorem 6.8 (Asymptotic properties of predictive online forward-backward splitting). For all $k \in \mathbb{N}$ and $\delta > 0$, suppose $F_{k+1}^\delta, G_{k+1}^\delta : X_{k+1} \rightarrow [0, \infty]$ are convex, proper, and lower semicontinuous, and the primal predictor $A_k^\delta : X_k \rightarrow X_{k+1}$. Let $\mathcal{B} \subset \prod_{k=0}^\infty X_k$ be bounded and suppose Assumption 6.3 holds. For every $\delta > 0$, for an initial iterate $x^0 = x_\delta^0 \in X_0$ independent of δ , generate $x_\delta^{1:\infty}$ by Algorithm 3.1. Assume for all $k \in \mathbb{N}$:

- (i) The prediction bound (3.2) holds with $\limsup_{N \rightarrow \infty, \delta \searrow 0} \frac{1}{N} \sum_{k=1}^N \varepsilon_k^\delta = 0$.
- (ii) The condition (3.5) and $\Lambda_k^\delta \leq 1 + \gamma_k^\delta \tau$ hold for $\tau_k \equiv \tau$ and $\zeta_k \equiv \zeta \geq 1$ independent of δ .

Then there exist $\bar{N}(\delta) \geq 1$ such that (6.10) holds. If $\zeta > 1$, then, moreover,

$$(6.11) \quad \lim_{\delta \searrow 0} \sup_{N \geq \bar{N}(\delta)} \frac{1}{2N} \sum_{k=0}^{N-1} \|x_\delta^{k+1} - A_k(x_\delta^k)\|^2 = 0.$$

Proof. We use Corollary 3.5, whose conditions we have assumed. Since $G_{k+1}^\delta(x_\delta^{k+1}) \geq 0$, minding (6.9), we thus obtain for all $\delta > 0$ and $N \geq 1$ that

$$(6.12) \quad R_N^\delta(x_\delta^{1:N}) + \sum_{k=0}^{N-1} \frac{1-\zeta}{2\tau N} \|x_\delta^{k+1} - A_k(x_\delta^k)\|^2 \leq e_{N,\delta} := \frac{1}{N\tau} \left(\sup_{\bar{x}^0 \in \mathcal{B}_0} \frac{1}{2} \|x^0 - \bar{x}^0\|^2 + \sum_{k=1}^N \varepsilon_k^\delta \right).$$

We have $e_{N,\delta} \rightarrow 0$ as $\delta \rightarrow 0$ and $N \rightarrow \infty$. Thus (6.3) holds. We verify (6.6) using (6.8) and $F_k^\delta \geq 0$. Lemmas 6.1 and 6.2 now establish (6.4) and (6.7) for some $\bar{N}(\delta) \geq 1$. As in the proof of Theorem 6.6, (6.7) and Assumption 6.3 imply (6.10) while (6.4) yields (6.11) from (6.12). \square

Theorem 6.9 (Asymptotic properties of predictive online primal-dual splitting). For all $k \in \mathbb{N}$ and $\delta > 0$, suppose $F_{k+1}^\delta : X_{k+1} \rightarrow [0, \infty]$ and $G_{k+1}^\delta, \tilde{G}_{k+1}^\delta : Y_{k+1} \rightarrow [0, \infty]$ are convex, proper, and lower semicontinuous, $K_{k+1}^\delta \in \mathbb{L}(X_{k+1}; Y)$, and the primal and dual predictors $A_k^\delta : X_k \rightarrow X_{k+1}$ and $B_k^\delta : Y_k \rightarrow Y_{k+1}$. Let the sets \mathcal{B} and \mathcal{U} be as in (5.3). For every $\delta > 0$, for an initial iterate $u^0 = u_\delta^0$ independent of δ , generate $u_\delta^{1:\infty}$ by Algorithm 5.1. Assume:

- (i) Assumption 6.3 holds for F_{k+1}^δ and $\tilde{G}_{k+1}^\delta := G_{k+1}^\delta \circ K_{k+1}^\delta$.
- (ii) For $\tilde{G}_{1:N}^\delta$ defined as in (5.15), $\frac{1}{N} \tilde{G}_{1:N}^\delta(K_{1:N}^\delta x_\delta^{1:N}) \geq -c_\delta$ with $c_\delta \rightarrow 0$ as $\delta \rightarrow 0$.
- (iii) The prediction bounds (5.5) hold with $\limsup_{\delta \rightarrow 0, N \rightarrow \infty} \frac{1}{N} \sum_{k=0}^{N-1} (\varepsilon_{k+1}^\delta + \tilde{\varepsilon}_{k+1}^\delta) = 0$. Moreover, $\rho_k^\delta \leq \bar{\rho}$ and $\Theta_k^\delta \geq \underline{\Theta}$ for some $\bar{\rho}, \underline{\Theta} > 0$.
- (iv) The step length parameters are as in Example 5.5, independent of δ and k .

Then there exist $\bar{N}(\delta) \geq 1$ verifying (6.10). If $\sup_{k \in \mathbb{N}, \delta > 0} \tau \sigma \|K_{k+1}^\delta\| < 1$, then also (6.11) holds.

Proof. Example 5.5 verifies the step length conditions (5.6) with $\eta_k \equiv \tau$, $\varphi_k \equiv 1$, and $\psi_k \equiv \frac{\tau}{\sigma}$. Minding (5.8), for all $\delta > 0$ and $N \geq 1$,

$$\|u_\delta^{k+1} - S_k^\delta(u_\delta^k)\|_{Z_{k+1}M_{k+1}}^2 \geq (1 - \tau \sigma \|K_{k+1}^\delta\|^2) \|x_\delta^{k+1} - A_k^\delta(x_\delta^k)\|^2.$$

Since $\tilde{G}_{1:N}^\delta(K_{1:N}^\delta x_\delta^{1:N}) \geq -c_\delta$,

$$R_N^\delta(x_\delta^{1:N}) - \frac{c_\delta}{N} \leq \sup_{\bar{x}^{1:N} \in \mathcal{B}_{1:N}} \frac{1}{N} \left([F_{1:N}^\delta + \tilde{G}_{1:N}^\delta \circ K_{1:N}^\delta](x_\delta^{1:N}) - [F_{1:N}^\delta + G_{1:N}^\delta \circ K_{1:N}^\delta](\bar{x}^{1:N}) \right).$$

Hence Theorem 5.8 bounds

$$(6.13) \quad R_N^\delta(x_\delta^{1:N}) + \sum_{k=0}^{N-1} \frac{1 - \tau \sigma \|K_{k+1}^\delta\|^2}{2N} \|x_\delta^{k+1} - A_k^\delta(x_\delta^k)\|^2 \leq e_{N,\delta} + \frac{c_\delta}{N}$$

$$\text{where } e_{N,\delta} := \sup_{\bar{u}^0 \in \mathcal{U}_0} \frac{1}{2N} \|\bar{u}^0 - \bar{u}^0\|_{Z_0 M_0 + \Gamma_0}^2 + \frac{1}{N} \sum_{k=0}^{N-1} \left(\varepsilon_{k+1}^\delta + \frac{\delta(1 + \sigma \bar{\rho})\tau}{2\underline{\Theta}\sigma} \tilde{\varepsilon}_{k+1}^\delta \right).$$

Example 5.5 ensures $\tau \sigma \|K_{k+1}^\delta\| \leq 1$, so using (ii) and (iii) this shows (6.3). We verify (6.6) using (6.8) and that $\tilde{J}_N^\delta \geq 0$ due to $F_k^\delta \geq 0$. Lemmas 6.1 and 6.2 now establish (6.4) and (6.7) for some $\bar{N}(\delta) \geq 1$. As in the proof of Theorem 6.6, (6.7) and Assumption 6.3 imply (6.10) while (6.4) yields (6.11) from (6.13). \square

Example 6.10 (Norm regularisation in POPD). For all $k \geq 1$, suppose $G_k^\delta = \alpha(\delta) \delta_{B_Y}^*$ for a bounded set B_Y on a Hilbert space Y . Then $(G_k^\delta)^* = \delta_{\alpha(\delta)B_Y}$ and Lemma 4.6 now shows that

$$\tilde{G}_{1:N}^\delta(\tilde{y}^{1:N}) \geq -G_{1:N}^\delta(\tilde{y}^{1:N}) = -\alpha(\delta) \sum_{k=1}^N \delta_{B_Y}^*(-\tilde{y}^k) \quad (\tilde{y}^{1:N} \in Y^N).$$

If $\{x_\delta^k\}_{k \in \mathbb{N}, \delta > 0}$ is bounded, then this shows that $\frac{1}{N} \tilde{G}_{1:N}^\delta(K_{1:N}^\delta x_\delta^{1:N}) \geq -C\alpha(\delta)$ for some $C > 0$ so that Theorem 6.9 (ii) holds when we choose $\alpha(\delta) \rightarrow 0$ as $\delta \rightarrow 0$.

7 OPTICAL FLOW

We now apply the previous sections to optical flow. For numerical accuracy, we use the more fundamental displacement field model instead of the linearised PDE model (transport equation). For simplicity, and to keep the static problems convex, we concentrate on constant-in-space (but not time) displacement fields. This makes our work applicable to computational image stabilisation (shake reduction) in still or video cameras, compare [30, 39], based on rapid successions of very noisy images. We start in Section 7.1 with a known displacement field—as could be estimated using acceleration sensors on cameras. Afterwards in Section 7.2 we include the estimation of the displacement field into our model.

7.1 KNOWN DISPLACEMENT FIELD

We start by assuming to be given in each frame, i.e., on each iteration, a noisy measurement $b_\delta^k \in X$ of a true image $\bar{b}^k \in X$ and a noisy measurement $v_\delta^k \in V$ of a true displacement field $\bar{v}^k \in V$. The measured displacement fields we assume bijective. The finite-dimensional subspaces $X \subset L^2(\Omega)$, $Y \subset L^2(\Omega; \mathbb{R}^2)$, and $V \subset L^2(\Omega; \Omega) \cap C^2(\Omega; \Omega)$ on a domain $\Omega \subset \mathbb{R}^2$ we equip with the L^2 -norm. To write (1.3) in min-max form, we take

$$(7.1a) \quad F_k^\delta(x) := \frac{1}{2} \|b_\delta^k - x\|_X^2, \quad (G_k^\alpha)^*(y) := \delta_{\alpha B}(y), \quad \text{and} \quad K_k = D,$$

for B the product of pointwise unit balls and $D : X \rightarrow L^2(\Omega)$ a discretised differential operator. For the primal and dual predictors we take

$$(7.1b) \quad A_k^\delta(x) := x \circ v_\delta^k \quad \text{and} \quad B_k^\delta(y) := y \circ v_\delta^k,$$

In the dual predictor of the POPD, we take $\tilde{G}_k^* = (G_k^\alpha)^* + \frac{\tilde{\rho}_k}{2} \|\cdot\|_{L^2(\Omega)}^2$ following Example 5.1. Thus \tilde{G}_k^* is the Fenchel conjugate of the Huber/Moreau–Yosida-regularised 1-norm.

REGARDING THE REGRET AND REGULARISATION THEORY

Let the true displacement fields $\bar{v}^k \in H^1(\mathbb{R}^2; \mathbb{R}^2)$, ($k \in \mathbb{N}$), and let $\mathcal{U}_0 \subset X \times Y$ be bounded. Following (5.3), we take for some $M > 0$,

$$\mathcal{U} := \left\{ \bar{u}^{0:\infty} \left| \begin{array}{l} \bar{u}^0 \in \mathcal{U}_0, \bar{x}^{k+1} = \bar{x}^k \circ \bar{v}^k, \bar{x}^k \in H^1(\mathbb{R}^2), \bar{y}^k \in H^1(\mathbb{R}^2; \mathbb{R}^2), \|\nabla \bar{y}^k\|_{2,\infty}^2 \leq M, \\ \|\nabla \bar{x}^k\|_{2,\infty}^2 \leq M, \bar{y}^{k+1} = \text{prox}_{\tilde{\sigma}_{k+1} \tilde{G}_{k+1}^*}(\bar{y}^k \circ \bar{v}^k + \tilde{\sigma}_{k+1} K_{k+1} \bar{x}^{k+1}), \forall k \geq 0 \end{array} \right. \right\}$$

as the comparison set. With a slight abuse notation we also write \mathcal{U} for the corresponding set with the domain of each \bar{u}^k restricted to Ω . We assume that the ground-truth images

$$\bar{b}^{0:\infty} \in \mathcal{B} := \{\bar{x}^{0:\infty} \mid \bar{u}^{0:\infty} \in \mathcal{U}\}.$$

Because the iterates y^k are in a finite-dimensional subspace, bounding $\|\nabla \bar{y}^k\|_{2,\infty}^2$ is no difficulty.

To satisfy (5.5a), we need to find factors $\Lambda_k^\delta \geq 0$ and penalties $\varepsilon_{k+1}^\delta \in \mathbb{R}$ such that

$$(7.2) \quad \frac{1}{2} \|x_\delta^k \circ v_\delta^k - \bar{x}^k \circ \bar{v}^k\|_X^2 \leq \frac{\Lambda_k^\delta}{2} \|x_\delta^k - \bar{x}^k\|_X^2 + \varepsilon_{k+1}^\delta \quad (\bar{x}^k \in \mathcal{B}_k).$$

The satisfaction of (5.5b) is handled analogously. If we had no displacement field measurement error, i.e., $v_\delta^k = \bar{v}^k$, we could by the area formula take $\Lambda_k^\delta = \max_{\xi \in \Omega} |\det \nabla (v_\delta^k)^{-1}(\xi)|$ and $\varepsilon_{k+1}^\delta = 0$. Otherwise we need the more elaborate estimate of the next lemma.

Lemma 7.1. Let $\bar{v} \in H^1(\mathbb{R}^2; \mathbb{R}^2)$ and $\bar{x} \in H^1(\Omega)$ with $\|\nabla \bar{x}\|_{2,\infty}^2 \leq M$ for some $M > 0$. Let $\mathcal{V} \subset H^1(\Omega; \Omega)$ be a set of bijective displacement fields satisfying

$$(7.3) \quad \Lambda_{\mathcal{V}} := \sup_{v \in \mathcal{V}, \xi \in \Omega} |\det \nabla v^{-1}(\xi)| < \infty.$$

Then for any $x \in L^2(\Omega)$, $v \in \mathcal{V}$, and $\Lambda > \Lambda_{\mathcal{V}}$,

$$\frac{1}{2} \|x \circ v - \bar{x} \circ \bar{v}\|_{L^2(\Omega)}^2 \leq \frac{\Lambda}{2} \|x - \bar{x}\|_{L^2(\Omega)}^2 + \frac{\Lambda_{\mathcal{V}}(4\Lambda - 3\Lambda_{\mathcal{V}})}{8(\Lambda - \Lambda_{\mathcal{V}})} M \|v - \bar{v}\|_{L^2(\Omega; \mathbb{R}^2)}^2.$$

Proof. By the area formula and Young's inequality, for any $t > 0$,

$$\begin{aligned} \int_{\Omega} |x(v) - \bar{x}(\bar{v})|^2 d\xi &\leq \int_{\Omega} \left(1 + \frac{t}{2}\right) |x(v(\xi)) - \bar{x}(v(\xi))|^2 + \left(1 + \frac{1}{2t}\right) |\bar{x}(v(\xi)) - \bar{x}(\bar{v}(\xi))|^2 d\xi \\ &= \left(1 + \frac{t}{2}\right) \int_{\Omega} |x(\xi) - \bar{x}(\xi)|^2 |\det \nabla v^{-1}(\xi)| d\xi + \left(1 + \frac{1}{2t}\right) \int_{\Omega} |\bar{x}(v) - \bar{x}(\bar{v})|^2 d\xi. \end{aligned}$$

Using (7.3) and that \bar{x} is \sqrt{M} -Lipschitz, it follows

$$\|x \circ v - \bar{x} \circ \bar{v}\|_{L^2(\Omega)}^2 \leq \left(1 + \frac{t}{2}\right) \Lambda_{\mathcal{V}} \|x - \bar{x}\|_{L^2(\Omega)}^2 + \left(1 + \frac{1}{2t}\right) M \|v - \bar{v}\|_{L^2(\Omega; \mathbb{R}^2)}^2.$$

Taking $t = 2(\Lambda/\Lambda_{\mathcal{V}} - 1)$ yields the claim. \square

We need the primal iterates to stay bounded. For this we use the next lemma:

Lemma 7.2. Compute x_{δ}^k and v_{δ}^k by Algorithm 5.1 for (7.1a) with fixed $\delta > 0$ and $\tau_k \equiv \tau > 0$. Suppose $\tau \leq \frac{(2-\Lambda)C-\varepsilon}{\alpha^2\|D\|^2}$ and $\|\xi_{\delta}^k - b_{\delta}^k\|^2 \leq C\Lambda + \varepsilon$ for some $C, \Lambda, \varepsilon > 0$. Then $\|x_{\delta}^k - b^k\|^2 \leq C$.

Proof. We drop the indexing by δ as it is fixed. The dual prediction of Algorithm 5.1 guarantees $\|v^k\|_{2,\infty} \leq \alpha$. The primal step is

$$(7.4) \quad x^k := \arg \min_x \|x - \xi^k - \tau Dv^k\|^2 + \tau \|x - b^k\|^2.$$

The optimality conditions are $0 = x^k - \xi^k + \tau Dv^k + \tau(x^k - b^k)$. Thus $\tau \|x^k - b^k\| = \|x^k - \xi^k + \tau Dv^k\|$. By (7.4), comparing to $x = \xi^k$, we get

$$2\|x^k - b^k\|^2 \leq \tau \|Dv^k\|^2 + \|\xi^k - b^k\|^2 \leq \tau \alpha^2 \|D\|^2 + C\Lambda + \varepsilon.$$

Thus $\|x^k - b^k\|^2 \leq C$ when τ is as stated. \square

We may now use Theorem 6.9 to prove convergence to the true data as the displacement field measurement error $\varepsilon \rightarrow 0$ along with the noise in the data b_{δ}^k .

Theorem 7.3. For all $k \in \mathbb{N}$, $\delta > 0$, and some $\alpha = \alpha(\delta) \rightarrow 0$ as $\delta \rightarrow 0$, assume the setup of (7.1) with $v_{\delta}^k \in \mathcal{V}$ for a set $\mathcal{V} \subset V$ of bijective displacement fields such that $\Lambda_{\mathcal{V}} < 2$. For an initial $u^0 = u_{\delta}^0$, for every $\delta > 0$, generate $u_{\delta}^{1:\infty}$ by Algorithm 5.1. With $\bar{b}^{0:\infty} \in \mathcal{B}$, assume:

- (I) $\sup_{k \in \mathbb{N}} \|b_{\delta}^k - \bar{b}^k\|_{L^2(\Omega)} \rightarrow 0$ and $\sup_{k \in \mathbb{N}} \|v_{\delta}^k - \bar{v}^k\|_{L^2(\Omega; \mathbb{R}^2)} \rightarrow 0$ as $\delta \rightarrow 0$.
- (II) For some $\Lambda_k, \Theta_k > \Lambda_{\mathcal{V}}$, the step length parameters are as in Example 5.5, independent of δ and k .

Then there exist $\bar{N}(\delta) \in \mathbb{N}$ such that $\lim_{\delta \rightarrow 0} \sup_{N \geq \bar{N}(\delta)} \frac{1}{N} \sum_{k=1}^N \|x_{\delta}^k - \bar{b}^k\|_{L^2(\Omega)}^2 = 0$. If $\tau \sigma \|D\|^2 < 1$ then, moreover, $\lim_{\delta \rightarrow 0} \sup_{N \geq \bar{N}(\delta)} \frac{1}{2\tau N} \sum_{k=0}^{N-1} \|x_{\delta}^{k+1} - x_{\delta}^k \circ v_{\delta}^k\|_{L^2(\Omega)}^2 = 0$.

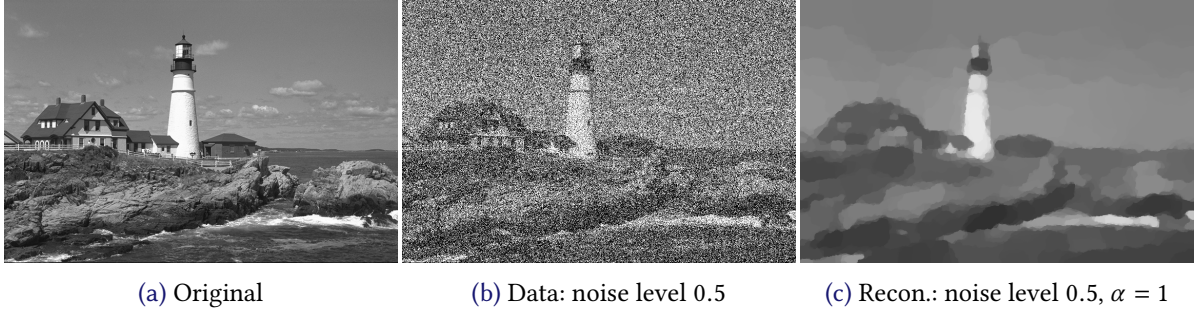


Figure 1: Lighthouse test image, added noise, and stationary reconstruction for comparison purposes

Proof. We first show the boundedness of $\{x_\delta^k\}_{k \in \mathbb{N}, \delta \in (0, \bar{\delta})}$ for some $\bar{\delta} > 0$. By (I), $\sup_{k \in \mathbb{N}} \|b_\delta^k - \bar{b}^k\|_X =: \delta_b \rightarrow 0$ and $\sup_{k \in \mathbb{N}} \|v_\delta^k - \bar{v}^k\|_{L^2(\Omega; \mathbb{R}^2)} =: \delta_v \rightarrow 0$ as $\delta \searrow 0$. We have $\bar{b}^{k+1} = \bar{b}^k \circ \bar{v}^k$ and $\xi_\delta^{k+1} = x_\delta^k \circ v_\delta^k$. Using Young's inequality twice for any $\beta > 0$ and Lemma 7.1 for any $\Lambda' > \Lambda_V$,

$$\begin{aligned} \|\xi_\delta^{k+1} - b_\delta^{k+1}\|_{L^2(\Omega)}^2 &\leq (1 + \beta) \|x_\delta^k \circ v_\delta^k - \bar{b}^k \circ \bar{v}^k\|_{L^2(\Omega)}^2 + (1 + \beta^{-1}) \|b_\delta^{k+1} - \bar{b}^k \circ \bar{v}^k\|_{L^2(\Omega)}^2 \\ &\leq \Lambda'(1 + \beta) \|x_\delta^k - \bar{b}^k\|_{L^2(\Omega)}^2 + (1 + \beta^{-1}) \delta_b^2 + (1 + \beta) \frac{\Lambda_V(4\Lambda' - 3\Lambda_V)}{8(\Lambda' - \Lambda_V)} M \delta_v^2 \\ &\leq \Lambda'(1 + \beta)^2 \|x_\delta^k - b_\delta^k\|_{L^2(\Omega)}^2 + (1 + \beta^{-1}) (\Lambda'(1 + \beta) + 1) \delta_b^2 + (1 + \beta) \frac{\Lambda_V(4\Lambda' - 3\Lambda_V)}{8(\Lambda' - \Lambda_V)} M \delta_v^2. \end{aligned}$$

Taking $\beta > 0$, $\Lambda' > \Lambda_V$ small enough, we obtain for any $\Lambda \in (\Lambda_V, 2)$ that $\|\xi_\delta^{k+1} - b_\delta^{k+1}\|^2 \leq \Lambda \|x_\delta^k - b_\delta^k\|^2 + \varepsilon_\delta$ for some $\varepsilon_\delta \searrow 0$ as $\delta \searrow 0$. By Lemma 7.2, now $\sup_k \|x_\delta^k - b_\delta^k\|^2 \leq C$ for any $C \geq \|x^0 - b^0\|^2$ with $\tau \leq \frac{(2-\Lambda)C - \varepsilon_\delta}{\alpha^2 \|D\|^2}$. This holds for C large and $\delta \in (0, \bar{\delta})$ for small $\bar{\delta} > 0$.

We base the rest of our proof on Theorem 6.9 whose assumptions we need to verify. Firstly, the structural setup and (i), i.e., Assumption 6.3, are clear from the choices (7.1), $\bar{b}^{0:\infty} \in \mathcal{B}$ and (I) with Examples 6.4 and 6.5. Secondly, (ii) follows from Example 6.10 and the boundedness of $\{x_\delta^k\}_{k \in \mathbb{N}, \delta \in (0, \bar{\delta})}$. Thirdly, (iii) is guaranteed by the definition of \mathcal{U} , Lemma 7.1, and (I). Finally, (iv) we have directly assumed in (II). Theorem 6.9 now proves the existence of $\bar{N}(\delta) \geq 1$ such that (6.10) holds. After expansion this says $\lim_{\delta \searrow 0} \sup_{N \geq \bar{N}(\delta)} \frac{1}{N} \sum_{k=1}^N \|x_\delta^k - b_\delta^k\|^2 = 0$. Using (I) we obtain our first claim. Under the additional condition $\tau \sigma \|D\| < 1$, Theorem 6.9 proves (6.11), which after expansion gives our second claim. \square

NUMERICAL SETUP

We perform our experiments on a simple square image as well as the lighthouse image from the free Kodak image suite [16]; this is in Figure 1 along with a noisy version and comparison single-frame total variation reconstruction. The original size is 768×512 pixels. For our experiments, we pick a 300 × 200 subimage moving according to Brownian motion of standard deviation 2. Thus the displacement fields $\bar{v}^k(\xi) = \xi - \bar{u}^k$ with $\bar{u}^k \in \mathbb{R}^2$ are constant in space. To the subimage we add 50% Gaussian noise (standard deviation 0.5 with original intensities in [0, 1]). To construct the measured displacements available to the algorithm we add 5% Gaussian noise (standard deviation 0.05 $\|\bar{u}^k\|$) to the true displacements.²

We take the regularisation parameter $\alpha = 1$. Thus the corresponding full-image total variation reconstruction is in Figure 1c. To parametrise the POPD (Algorithm 5.1) we

² Then (7.3) gives $\Lambda_V = 1$. Constant true displacements are allowed by Lemma 7.1, but constant measurements not. If $\|x - \bar{x}\|_{L^2(\Omega+B(0, \|u\|))}^2 \leq C \|x - \bar{x}\|_{L^2(\Omega)}^2$ then Lemma 7.1 and Theorem 7.3 extend to $\Lambda > C\Lambda_V$. In practise, to compute $x \circ v$, we extrapolate x outside Ω such that Neumann boundary conditions are satisfied.

- Fix the primal step length parameter $\tau = 0.01$ as well as $\Lambda = \Theta = 1$ and $\kappa = 0.9$.
- Take the primal strong convexity factor $\gamma = 1$ and generally the dual factor $\rho = 0$.
- Take $\tilde{\sigma}$, maximal σ , and minimal $\hat{\rho}_{k+1} \equiv \hat{\rho}$ according to [Example 5.5](#). Here we estimate $\|K_k\| \leq \sqrt{8}$ for forward-differences discretisation of $K_k = D$ with cell width $h = 1$ [10].

Although G_{k+1}^* is not strongly convex, we also experiment taking a “phantom” $\rho = 100$. This can in principle be justified via *local* strong convexity or *strong metric subregularity* at a solution. We briefly indicate how this works in [Appendix A](#). The effect in practise is to increase the dual step length parameter σ . We always take zero as the initial iterate (primal and dual).

We implemented our algorithms in Julia 1.3 [7], and performed our experiments on a mid-2014 MacBook Pro with 16GB RAM. The implementation is available on Zenodo [35].

NUMERICAL RESULTS

We display the reconstructions in [Figures 2 to 4](#) and the performance (function value, PSNR, and SSIM) in [Figures 6a, 7a and 8a](#). The reconstructions are for the frames/iterations 30, 50, 100, 300, 500, 1000, and 3000 whereas the performance plots display all 10000 iterations at a resolution of 100 iterations after the first 100 iterations. The right-most column of the reconstruction figures displays the true cumulative displacement field up to the corresponding data frame (indicated in the bottom-left corner). The darker line is sampled at the same resolution as the performance plots whereas the lighter line is sampled at every iteration. Regarding real-time computability, averaged over the 10000 iterations, every iteration takes ~ 6.5 ms, which is to say the POPD can process 154 frames per second.

The performance plots show convergence of the function value to a stable value, not necessarily a minimum, within 100 iterations. Likewise the SSIM and PSNR reach a relatively stable and acceptable value by 100 iterations. Visually, we have decent tracking of movement, but we need the large ρ -value to get a noticeable cartoon-like “total variation effect”. In the last frame of [Figure 2](#) we can see the effect of the algorithm not being able to track a sudden large displacement fast enough, hence producing some motion blur. The 100 iterations, that were needed to reach a stable function value, SSIM, or PSNR, appear to be mainly needed to reach the correct contrast level: recall that we initialise with zero. We tested initialising the primal variable with the noisy data: the algorithm then needed a similar number of iterations to reduce the noise. A smarter initialisation might help reduce the 100-iteration “initialisation window”.

For comparison, we have included POFB reconstruction ([Algorithm 3.1](#)) in [Figure 5](#). We use the step length parameter $\tau = 0.01$ for the POFB itself. We take 10 iterations of FISTA [4] with step length parameter $\tilde{\tau} = 1/\|K\|^2$ to approximately solve the proximal step. By the performance measures the results are comparable to the POPD. Visually they are similar to the high- ρ POPD. The algorithm is, however, quite a bit slower: ~ 21.2 ms/frame or 47 frames per second. Solving the proximal step accurately would further slow it down.

7.2 UNKNOWN DISPLACEMENT FIELD

When the displacement field v_k is completely unknown, we need to estimate it from data. For some $E_k : V \rightarrow \overline{\mathbb{R}}$ we do this through

$$(7.5) \quad \min_{x \in X, v \in V} \frac{1}{2} \|b_k - x\|_X^2 + \alpha \|Dx\| + E_k(v)$$

We drop the indexing by the noise level $\delta > 0$ as we will not be studying regularisation properties. Ideally we would take $E_k(v)$ as $\frac{\theta}{2} \|b^{k+1} - b^k \circ v\|_X^2$, plus regularisation terms. However, the resulting problem would be highly nonconvex. A second idea is to use a Horn–Schunck [21] type penalty on

linearised optical flow³, taking for some parameters $\theta, \lambda_1, \lambda_2 > 0$,

$$(7.6) \quad E_k(v) = \frac{\theta}{2} \|b_{k+1} - b_k + \langle \text{Id} - v, \nabla b_k \rangle\|_X^2 + \frac{\lambda_1}{2} \|\text{Id} - v\|_2^2 + \frac{\lambda_2}{2} \|\nabla v\|_2^2,$$

where the pointwise inner product $\langle a, b \rangle(\xi) := \langle a(\xi), b(\xi) \rangle$. We regularise the displacement field v to both be close to identity (no displacement) and to be smooth in space.⁴

The choice (7.6) is, however, very inaccurate in practise. We therefore, firstly, introduce a time-step parameter T and a convolution kernel ϱ to counteract noise in the data. Secondly, we average the Horn–Schunck term over a window of n frames. For iteration k , the last frame is

$$i(k) := \max\{1, k + 1 - (n - 1)\} \quad \text{and its true length} \quad n_k := k + 1 - (i(k) - 1).$$

With $j \in \{i(k), \dots, k + 1\}$, we write $v_j^k \in V$ for the displacement of b^j from $b^{i(k)-1}$ as estimated on iteration k . Then the displacement of b^{j+1} from b^j is $(v_j^k)^{-1} \circ v_{j+1}^k$. We take $E_k : V^{n_k+1} \rightarrow \mathbb{R}$,

$$(7.7) \quad E_k(v_{i(k):k+1}^k) := \frac{1}{n_k} \sum_{j=i(k)-1}^k \left(\frac{\theta}{2} \|\varrho * (b^{j+1} - b^j)/T + \langle \text{Id} - (v_j^k)^{-1} \circ v_{j+1}^k, \nabla(\varrho * b^j) \rangle\|_X^2 \right. \\ \left. + \frac{\lambda_1}{2} \|\text{Id} - (v_j^k)^{-1} \circ v_{j+1}^k\|_2^2 + \frac{\lambda_2}{2} \|\nabla v_j^k\|_2^2 \right).$$

Although not given as a parameter, we use $v_{i(k)-1}^k = 0$.

We predict the primal variables using

$$A_k(x, v_{i(k):k+1}^k) := \begin{cases} (x \circ (v_k^k)^{-1} \circ v_{k+1}^k, v_1^k, \dots, v_{k+1}^k, 0), & k < n, \\ (x \circ (v_k^k)^{-1} \circ v_{k+1}^k, (v_{i(k)}^k)^{-1} \circ v_{i(k+1)}^k, \dots, (v_{i(k)}^k)^{-1} \circ v_{k+1}^k, 0), & k \geq n, \end{cases}$$

and the dual variables using

$$B_k(y) := y \circ (v_k^k)^{-1} \circ v_{k+1}^k$$

Hence we a) propagate the image x and the dual variable using the estimated displacement of the next frame from the current frame, b) update the displacement estimates to be with respect to the start $i(k + 1)$ of the new n -frame window, and c) predict the displacement between the next two frames to be zero. The latter is consistent with the zero-mean Brownian motion used in our numerical experiments.

To write the problem (7.5) with E_k given by (7.7) in the saddle point form (1.6), we take

$$F_k(x, v_{i(k):k+1}^k) := \frac{1}{2} \|b^k - x\|_V^2 + E_k(v_{i(k):k+1}^k), \quad K_k(x, v_{i(k):k+1}^k) := Dx, \quad \text{and} \quad G_k^*(y) := \delta_{\alpha B}(y).$$

We split $\text{prox}_{\tau F_k}$ into individual updates with respect to x and $v_{i(k):k+1}^k$. If the displacement fields are constant in space, $v_j^k(\xi) = \xi - u_j^k$ with $u_j^k \in \mathbb{R}^2$, the compositions $(v_{i(k)}^k)^{-1} \circ v_j^k \equiv u_{i(k)}^k - u_j^k$, and $\text{prox}_{\tau E_k}$ reduces to an easily solvable chain of 2×2 quadratic optimisation problems.

The Horn–Schunck linearisation of the optical flow only converges to the true optical flow as we increase the temporal resolution. Therefore, we cannot directly apply the theory of Section 6 to obtain convergence of solutions generated by the POPD to a true solution as the noise level goes to zero: we would also need to increase the temporal resolution. We have, therefore, decided not to pursue any regret estimates. It is, however, not difficult to extend Lemma 7.1.

³To obtain the linearised optical flow model, we start with $b_{k+1}(\xi) = b_k(v_k(\xi))$ holding for all $\xi \in \Omega$ and a sufficiently smooth image b_k . By Taylor expansion $b_k(v_k(\xi)) \approx b_k(\xi) + \langle \nabla b_k(\xi), v_k(\xi) - \xi \rangle$. Thus $0 = b_{k+1}(\xi) - b_k(v_k(\xi)) \approx b_{k+1}(\xi) - b_k(\xi) + \langle \nabla b_k(\xi), \xi - v_k(\xi) \rangle$.

⁴Indeed, in linearised optical flow the displacement field cannot in general be discontinuous. See [31, 13] for approaches designed to avoid this restriction.

NUMERICAL SETUP AND RESULTS

For our numerical experiments we use generally the same setup as in Section 7.1 except we reduce the noise level in the image to 30% and correspondingly take $\alpha = 0.2$. For our new parameters we take $\lambda_1 = 1$ and $\theta = (300 \cdot 200) \cdot 100^3$ with constant-in-space displacement fields, so that λ_2 is irrelevant in (7.7). For the displacement estimation we use a window of $n = 100$ previous frames. For the smoothing kernel ρ in the Horn–Schnuck term of (7.7) we take a normalised Gaussian of standard deviation 3 pixels in a window of 11×11 pixels. We also take the time step parameter $T = 0.5$ for the lighthouse and $T = 1$ for the square test image. Our Julia implementation is available on Zenodo [35].

The reconstructions and estimated displacements are in Figures 9 to 11 and the performance plots (function value, PSNR, SSIM) in Figures 6b, 7b and 8b. Regarding real-time computability, the POPD requires 20.8ms/iteration, that is, can process 48 frames per second.

The function values take a long time to decrease. The PSNR and SSIM, however, again reach an acceptable and somewhat stable value after 100–200 iterations. Visually, the results are somewhat more blurred than with the approximately known displacement in Section 7.1, and even with $\rho = 100$ the cartoon-like total variation effect remains small. Nevertheless, the reconstructions are visually pleasing and the displacement is estimated to an acceptable accuracy. This did, however, require adapting the time-step parameter T to the test case. Improving the optical flow model to not require such an extraneous parameter is something for future research: we believe that the present results already demonstrate that online optimisation is a worthy approach to dynamic imaging.

8 CONCLUSION

With the goal of solving—for now relatively simple—imaging problems “online”, in real-time, we incorporated predictors into the forward-backward and primal-dual proximal splitting methods. For the predictive online forward-backward method (POFB) a reasonable notion of “dynamic regret” stays bounded, and can even converge below zero. Using regularisation theory we, moreover, proved convergence to a ground-truth as the level of corruption in the problem data vanishes. Hence the method forms an appropriate regulariser.

We do not, yet, understand the predictive online primal-dual method (POPD) as well. While we have shown analogous results, including convergence as the data improves, the form of “regret” we were able to employ still requires study and interpretation. This notwithstanding, our numerical results on optical flow are encouraging. More research is needed to understand the parametrisation and improved predictors needed to make the total variation effect prominent.

APPENDIX A LOCAL STRONG CONVEXITY

We establish local strong convexity of the indicator function of the ball. This has been shown in [1] to be equivalent to the *strong metric subregularity* of the subdifferential. For related characterisations, see also [32] and regarding total variation [23, appendix].

Lemma A.1. *With $F : X \rightarrow \mathbb{R}$, $F = \delta_{\text{cl} B(0, \alpha)}$ on a Hilbert space X , suppose $x \in \partial B(0, \alpha)$ and $0 \neq x^* \in \partial F(x)$. Then*

$$F(x') - F(x) \geq \langle x^*, x' - x \rangle + \frac{\gamma}{2} \|x' - x\|^2 \quad (x' \in U_x)$$

for

$$U_x = \begin{cases} X, & 0 \leq \gamma \alpha \leq \|x^*\|, \\ [\text{cl} B(0, \alpha)]^c \cup \text{cl} B(x, \alpha), & \alpha \gamma > \|x^*\|. \end{cases}$$

Proof. Observe that $x^* = \lambda x$ for $\lambda := \|x^*\|/\alpha$. If $x' \notin \text{cl } B(0, \alpha)$, there is nothing to prove. So take $x' \in \text{cl } B(0, \alpha)$. Then we need $0 \geq \lambda \langle x, x' - x \rangle + \frac{\gamma}{2} \|x' - x\|^2$. Since $\|x\| = \alpha$, this says

$$(A.1) \quad \left(\lambda - \frac{\gamma}{2}\right) \alpha^2 \geq \frac{\gamma}{2} \|x'\|^2 + (\lambda - \gamma) \langle x, x' \rangle.$$

Suppose $\gamma \leq \lambda$, which is the first case of U_x . Then (A.1) is seen to hold by application of Young's inequality on the inner product term, followed by $\|x'\| \leq \alpha$.

If on the other hand, $\gamma > \lambda$, which is the second case of U_x , we take $x' \in \text{cl } B(x, \alpha) \cap \text{cl } B(0, \alpha)$. This implies $\langle x', x \rangle \geq \frac{1}{2} \|x'\|^2$. Since $\lambda - \gamma < 0$, this and $\|x'\| \leq \alpha$ prove (A.1). \square

REFERENCES

- [1] F.J. Aragón Artacho and M.H. Geoffroy, Characterization of metric regularity of subdifferentials, *Journal of Convex Analysis* 15 (2008), 365–380.
- [2] N. Bastianello, A. Simonetto, and R. Carli, Prediction-Correction Splittings for Time-Varying Optimization With Intermittent Observations, *IEEE Control Systems Letters* 4 (2020), 373–378, doi:10.1109/lcsys.2019.2930491.
- [3] H.H. Bauschke and P.L. Combettes, *Convex Analysis and Monotone Operator Theory in Hilbert Spaces*, CMS Books in Mathematics, Springer, 2 edition, 2017, doi:10.1007/978-3-319-48311-5.
- [4] A. Beck and M. Teboulle, A Fast Iterative Shrinkage-Thresholding Algorithm for Linear Inverse Problems, *SIAM Journal on Imaging Sciences* 2 (2009), 183–202, doi:10.1137/080716542.
- [5] F. Becker, S. Petra, and C. Schnörr, Optical Flow, in *Handbook of Mathematical Methods in Imaging*, O. Scherzer (ed.), Springer, 2015, 1945–2004, doi:10.1007/978-1-4939-0790-8_38.
- [6] E.V. Belmega, P. Mertikopoulos, R. Negrel, and L. Sanguinetti, Online convex optimization and no-regret learning: Algorithms, guarantees and applications, 2018, arXiv:804.04529.
- [7] J. Bezanson, A. Edelman, S. Karpinski, and V.B. Shah, Julia: A fresh approach to numerical computing, *SIAM Review* 59 (2017), 65–98, https://doi.org/10.1137/141000671.
- [8] L. Biegler, O. Ghattas, M. Heinkenschloss, D. Keyes, and B. Waanders, *Real-Time PDE-Constrained Optimization*, Computational Science and Engineering, SIAM, 2007.
- [9] O. Bousquet and L. Bottou, The Tradeoffs of Large Scale Learning, *Advances in Neural Information Processing Systems* 20 (2008), 161–168, http://papers.nips.cc/paper/3323-the-tradeoffs-of-large-scale-learning.pdf.
- [10] A. Chambolle, An algorithm for total variation minimization and applications, *Journal of Mathematical Imaging and Vision* 20 (2004), 89–97, doi:10.1023/b:jmiv.0000011325.36760.1e.
- [11] A. Chambolle and T. Pock, A first-order primal-dual algorithm for convex problems with applications to imaging, *Journal of Mathematical Imaging and Vision* 40 (2011), 120–145, doi:10.1007/s10851-010-0251-1.
- [12] K. Chaudhury and R. Mehrotra, A trajectory-based computational model for optical flow estimation, *IEEE Transactions on Robotics and Automation* 11 (1995), 733–741, doi:10.1109/70.466611.
- [13] K. Chen and D.A. Lorenz, Image Sequence Interpolation Based on Optical Flow, Segmentation, and Optimal Control, *IEEE Transactions on Image Processing* 21 (2012), doi:10.1109/tip.2011.2179305.

- [14] C. Clason and T. Valkonen, Introduction to Nonsmooth Analysis and Optimization, 2020, [arXiv:2001.00216](https://arxiv.org/abs/2001.00216), https://tuomov.iki.fi/m/nonsmoothbook_part.pdf. Work in progress.
- [15] H. Engl, M. Hanke, and A. Neubauer, *Regularization of Inverse Problems*, Mathematics and Its Applications, Springer, 2000.
- [16] R. Franzen, Kodak lossless true color image suite, PhotoCD PCD0992. Lossless, true color images released by the Eastman Kodak Company, 1999, <http://rok.us/graphics/kodak/>.
- [17] M. Grötschel, S. Krumke, and J. Rambau, *Online Optimization of Large Scale Systems*, Springer Berlin Heidelberg, 2013.
- [18] E. Hall and R. Willett, Dynamical models and tracking regret in online convex programming, in *Proceedings of the 30th International Conference on Machine Learning*, S. Dasgupta and D. McAllester (eds.), volume 28 of Proceedings of Machine Learning Research, PMLR, Atlanta, Georgia, USA, 2013, 579–587, <http://proceedings.mlr.press/v28/hall13.html>.
- [19] E. Hazan, Introduction to Online Convex Optimization, *Foundations and Trends in Optimization* 2 (2016), 157–325, [doi:10.1561/24000000013](https://doi.org/10.1561/24000000013).
- [20] B. He and X. Yuan, Convergence Analysis of Primal-Dual Algorithms for a Saddle-Point Problem: From Contraction Perspective, *SIAM Journal on Imaging Sciences* 5 (2012), 119–149, [doi:10.1137/100814494](https://doi.org/10.1137/100814494).
- [21] B. K. Horn and B. G. Schunck, Determining Optical Flow, in *Proc. SPIE*, volume 0281, SPIE, 1981, 319–331, [doi:10.1117/12.965761](https://doi.org/10.1117/12.965761).
- [22] J. A. Iglesias and C. Kirisits, Convective regularization for optical flow, in *Variational Methods In Imaging and Geometric Control*, De Gruyter, 2016, 184–201, [doi:10.1515/9783110430394](https://doi.org/10.1515/9783110430394).
- [23] J. Jauhainen, P. Kuusela, A. Seppänen, and T. Valkonen, Relaxed Gauss–Newton methods with applications to electrical impedance tomography (2020). Work being finalised.
- [24] B. Kaltenbacher, Minimization Based Formulations of Inverse Problems and Their Regularization, *SIAM Journal on Optimization* 28 (2018), 620–645, [doi:10.1137/17m1124036](https://doi.org/10.1137/17m1124036).
- [25] H. H. Nagel, Extending the ‘Oriented smoothness constraint’ into the temporal domain and the estimation of derivatives of optical flow, in *Computer Vision—ECCV 90*, O. Faugeras (ed.), Springer Berlin Heidelberg, Berlin, Heidelberg, 1990, 139–148.
- [26] H. H. Nagel et al., Constraints for the Estimation of Displacement Vector Fields From Image Sequences, in *Proceedings of the Eighth International Joint Conference on Artificial Intelligence (II)*, volume 2, IJCAI, 1983, 945–951.
- [27] F. Orabona, A Modern Introduction to Online Learning, 2020, [arXiv:1912.13213](https://arxiv.org/abs/1912.13213).
- [28] A. Salgado and J. Sánchez, Temporal Constraints in Large Optical Flow Estimation, in *Computer Aided Systems Theory—EUROCAST 2007*, R. Moreno Díaz, F. Pichler, and A. Quesada Arencibia (eds.), Springer Berlin Heidelberg, Berlin, Heidelberg, 2007, 709–716.
- [29] A. Simonetto, Time-varying convex optimization via time-varying averaged operators, 2017, [arXiv:1704.07338](https://arxiv.org/abs/1704.07338).
- [30] M. Tico, Digital Image Stabilization, in *Recent Advances in Signal Processing*, A. A. Zaher (ed.), IntechOpen, Rijeka, 2009, chapter 1, [doi:10.5772/7458](https://doi.org/10.5772/7458).

- [31] T. Valkonen, Transport equation and image interpolation with SBD velocity fields, *Journal de mathématiques pures et appliquées* 95 (2011), 459–494, doi:10.1016/j.matpur.2010.10.010, <https://tuomov.iki.fi/m/bd.pdf>.
- [32] T. Valkonen, Preconditioned proximal point methods and notions of partial subregularity, 2017, [arXiv:1711.05123](https://arxiv.org/abs/1711.05123). submitted.
- [33] T. Valkonen, Testing and non-linear preconditioning of the proximal point method, *Applied Mathematics and Optimization* (2018), doi:10.1007/s00245-018-9541-6, [arXiv:1703.05705](https://arxiv.org/abs/1703.05705), <https://tuomov.iki.fi/m/proxtest.pdf>.
- [34] T. Valkonen, First-order primal-dual methods for nonsmooth nonconvex optimisation, 2019, [arXiv:1910.00115](https://arxiv.org/abs/1910.00115), <https://tuomov.iki.fi/m/firstorder.pdf>. submitted.
- [35] T. Valkonen, Julia codes for “Predictive online optimisation with applications to optical flow”, Online resource on Zenodo, 2020, doi:10.5281/zenodo.3659180.
- [36] S. Volz, A. Bruhn, L. Valgaerts, and H. Zimmer, Modeling temporal coherence for optical flow, in *2011 International Conference on Computer Vision*, IEEE, 2011, 1116–1123, doi:10.1109/iccv.2011.6126359.
- [37] J. Weickert and C. Schnörr, Variational Optic Flow Computation with a Spatio-Temporal Smoothness Constraint, *Journal of Mathematical Imaging and Vision* 14 (2001), 245–255, doi:10.1023/a:1011286029287.
- [38] Y. Zhang, R. J. Ravier, V. Tarokh, and M. M. Zavlanos, Distributed Online Convex Optimization with Improved Dynamic Regret, 2019, [arXiv:1911.05127](https://arxiv.org/abs/1911.05127).
- [39] J. Zhou, P. Hubel, M. Tico, A. N. Schulze, and R. Toft, Image registration methods for still image stabilization, US Patent 9,384,552, 2016.
- [40] M. Zinkevich, Online convex programming and generalized infinitesimal gradient ascent, in *Proceedings of the 20th International Conference on Machine Learning (ICML-03)*, AAAI, 2003, 928–936.

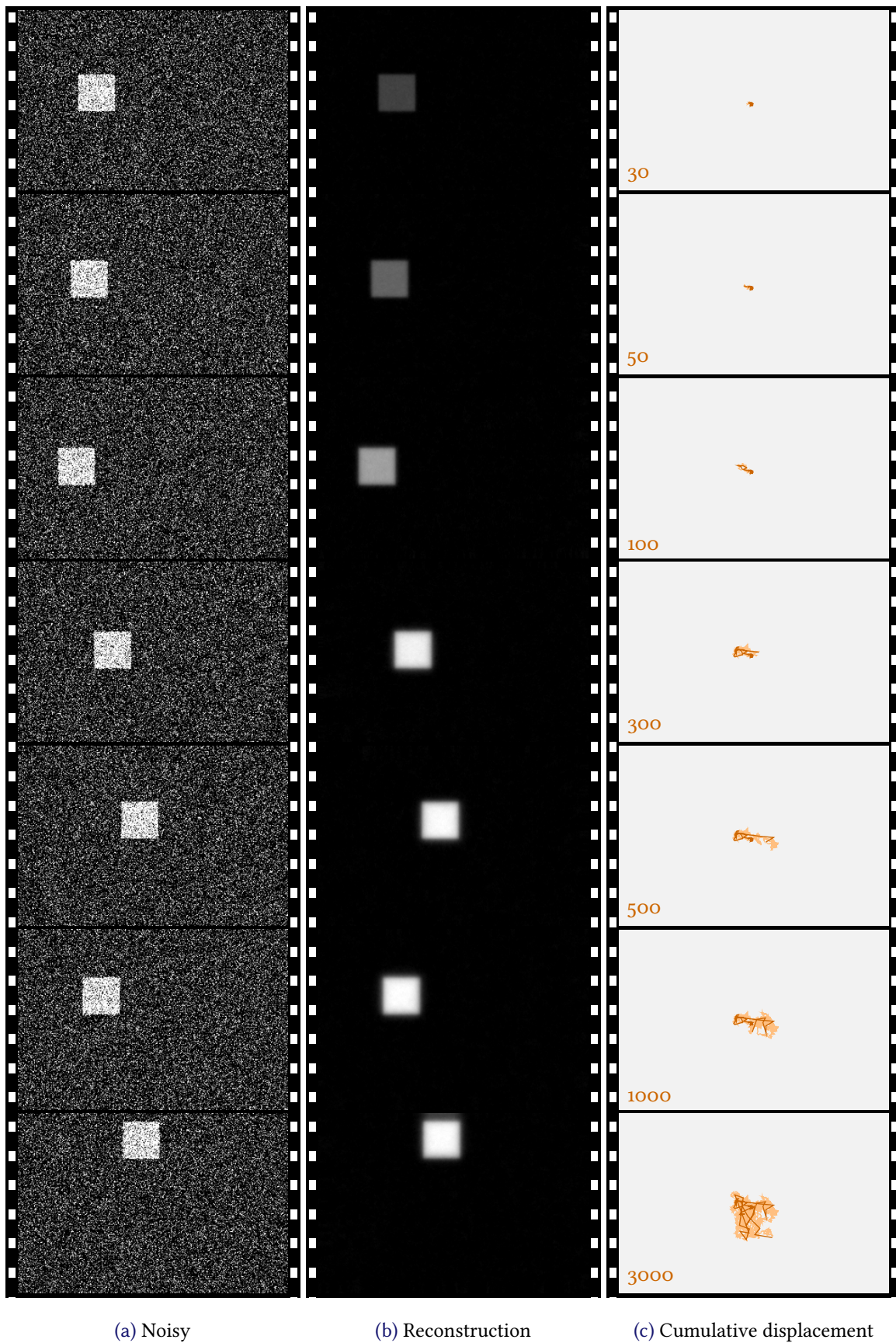
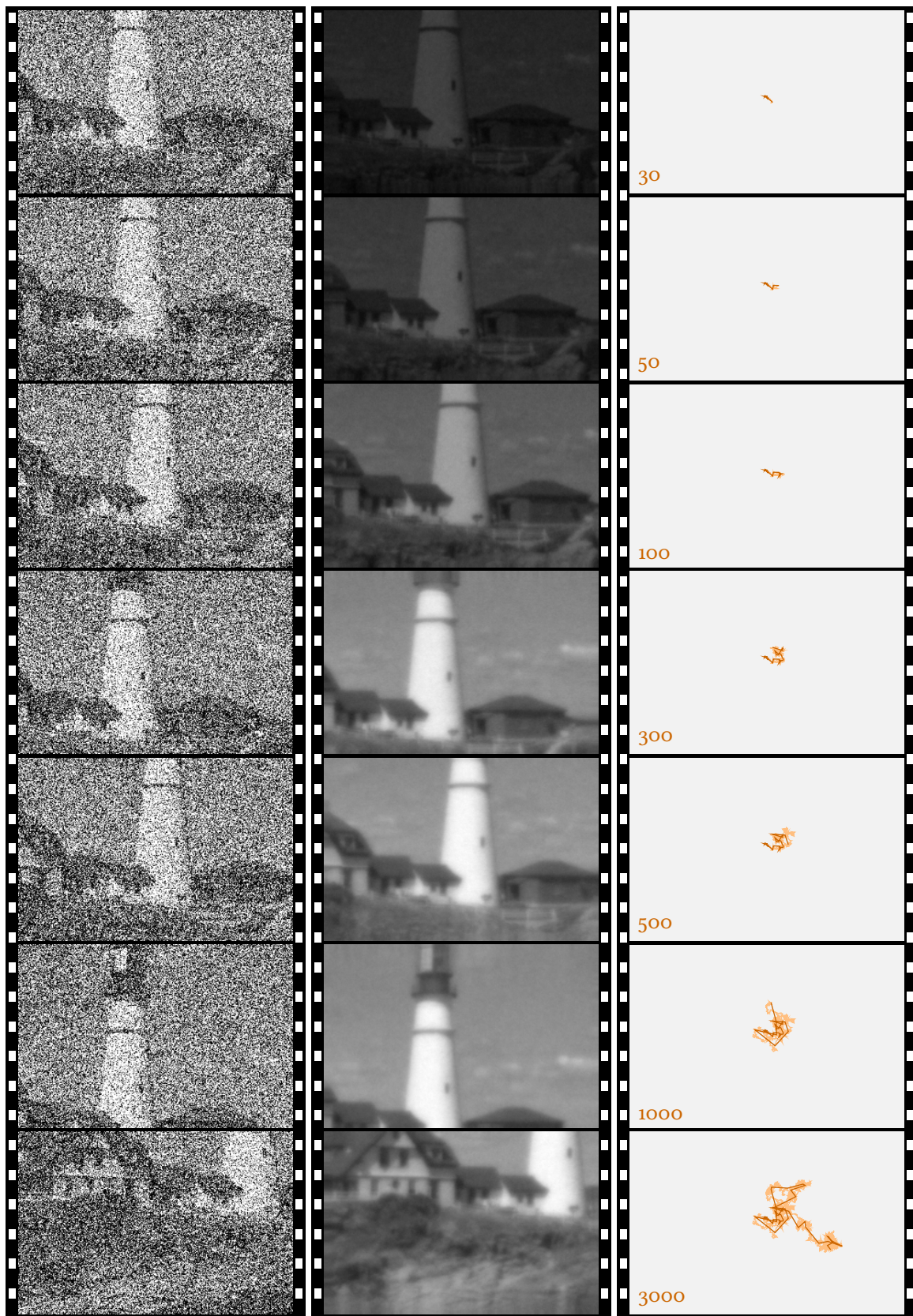


Figure 2: Square, POPD, approximately known displacement, $\rho = 0$.

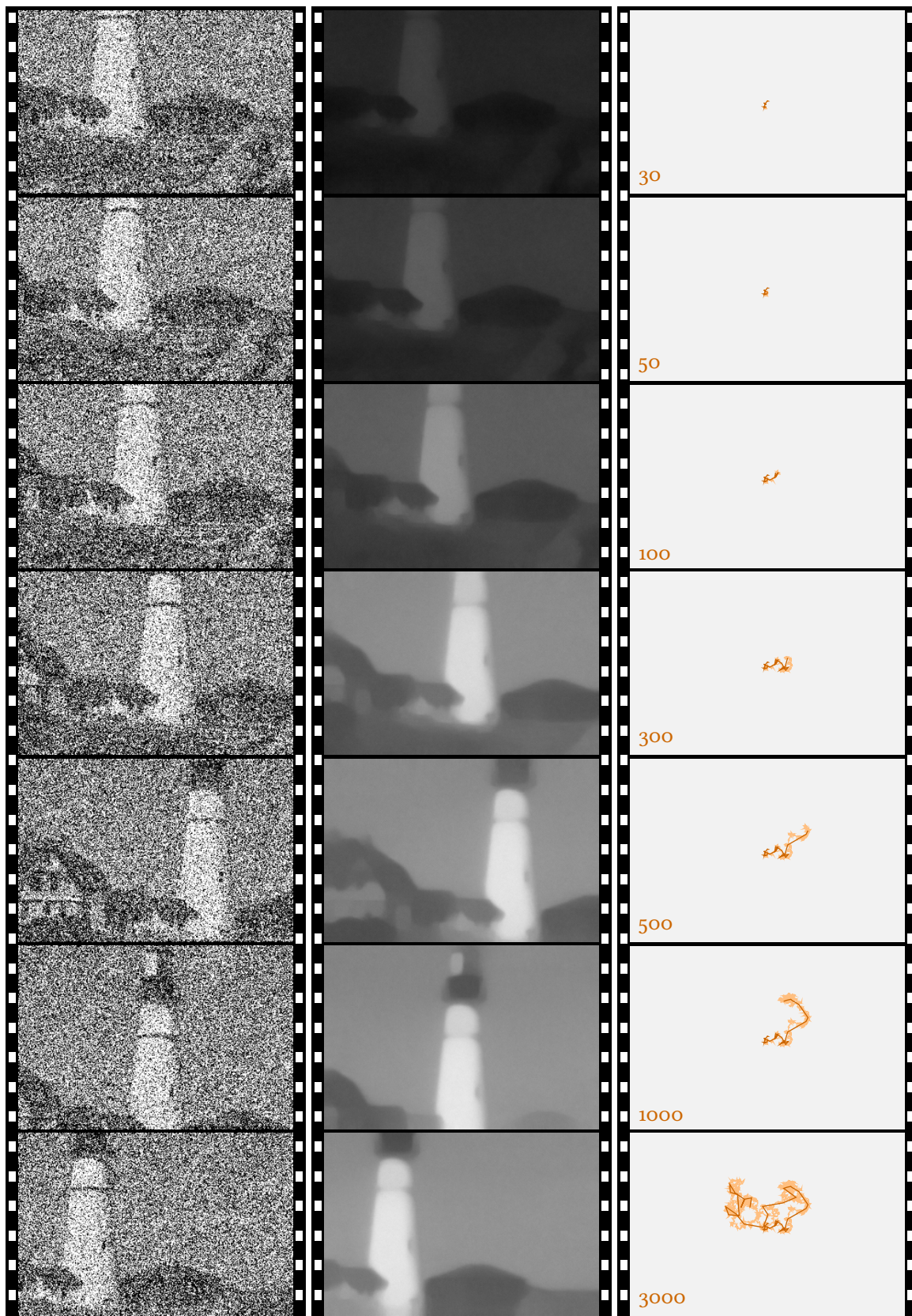


(a) Noisy

(b) Reconstruction

(c) Cumulative displacement

Figure 3: Lighthouse, POPD, approximately known displacement, $\rho = 0$.

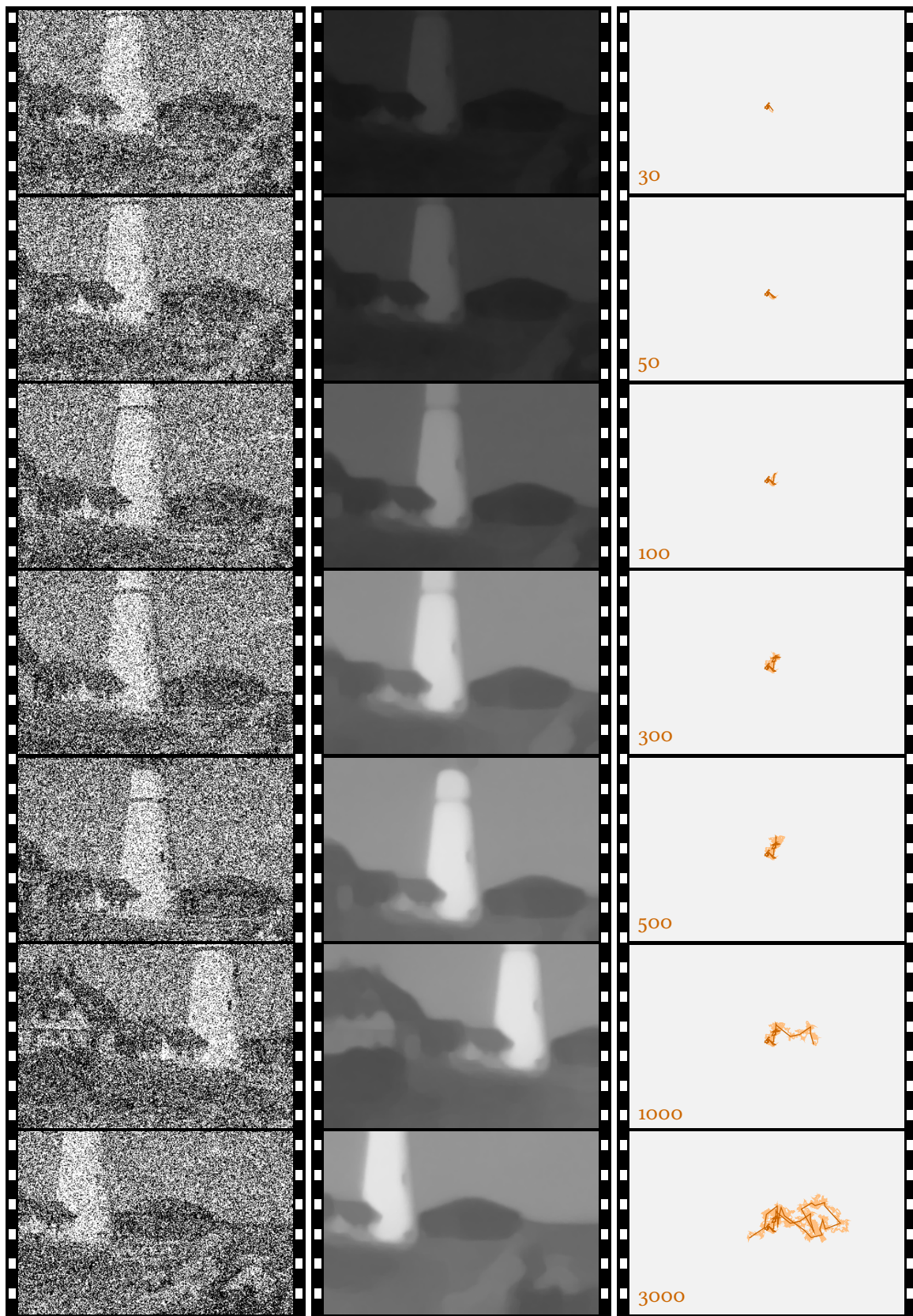


(a) Noisy

(b) Reconstruction

(c) Cumulative displacement

Figure 4: Lighthouse, POPD, approximately known displacement, $\rho = 100$.



(a) Noisy

(b) Reconstruction

(c) Cumulative displacement

Figure 5: Lighthouse, POFB, approximately known displacement.

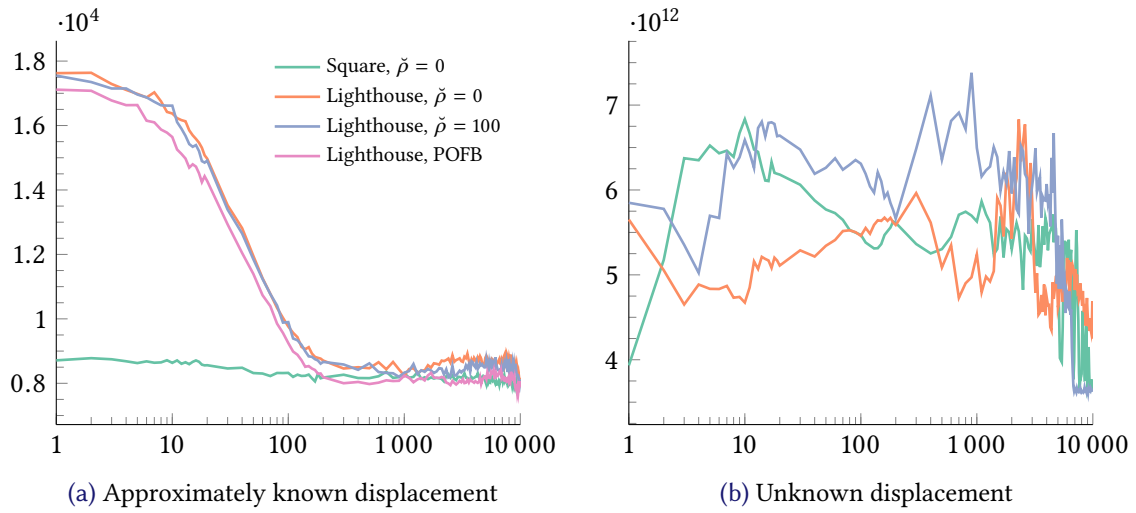


Figure 6: Iteration-wise objective values.

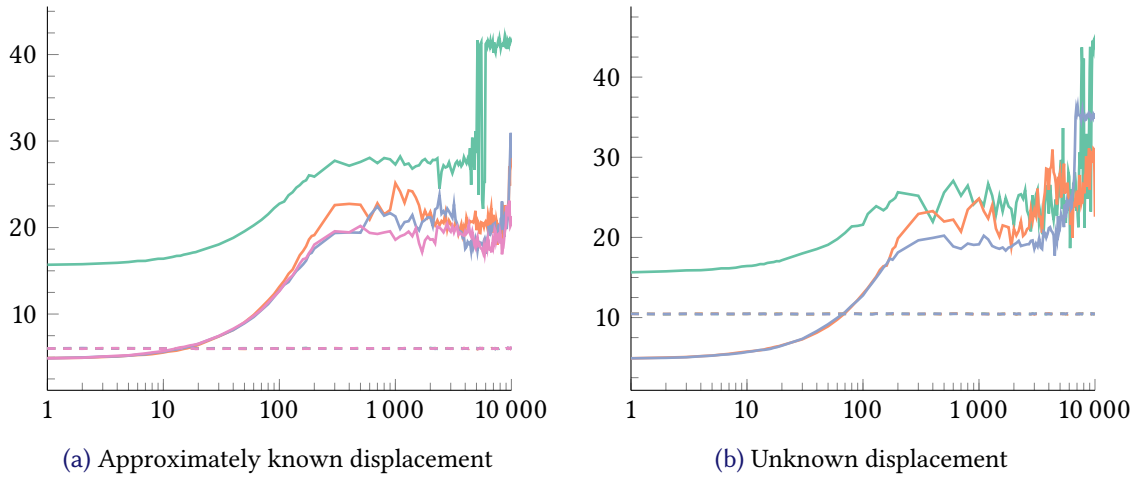


Figure 7: Iteration-wise PSNR. The dashed lines indicate the PSNR for the noisy data corresponding to the experiment of the solid line of the same colour. Legend in Figure 6a.

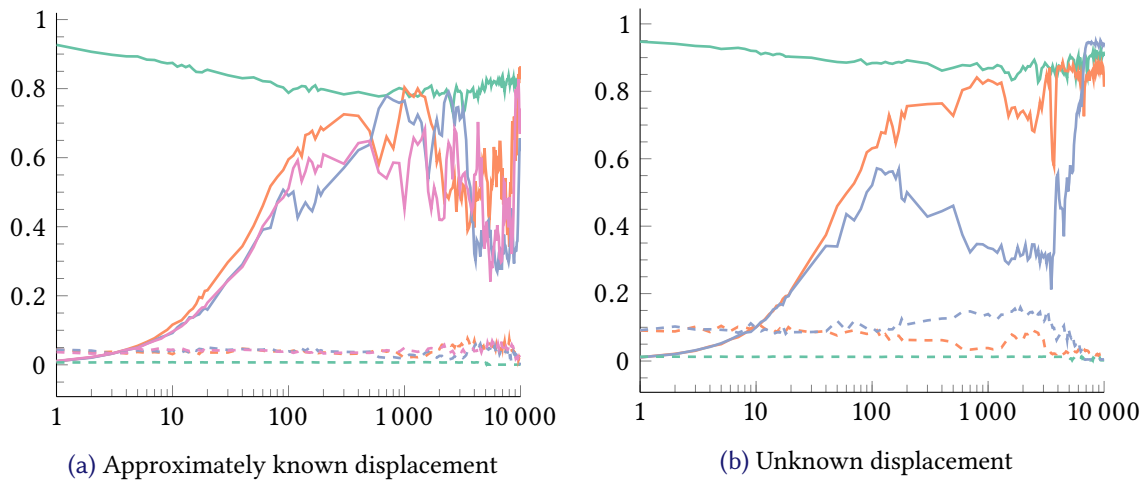


Figure 8: Iteration-wise SSIM. The dashed lines indicate the SSIM for the noisy data corresponding to the experiment of the solid line of the same colour. Legend in Figure 6a.

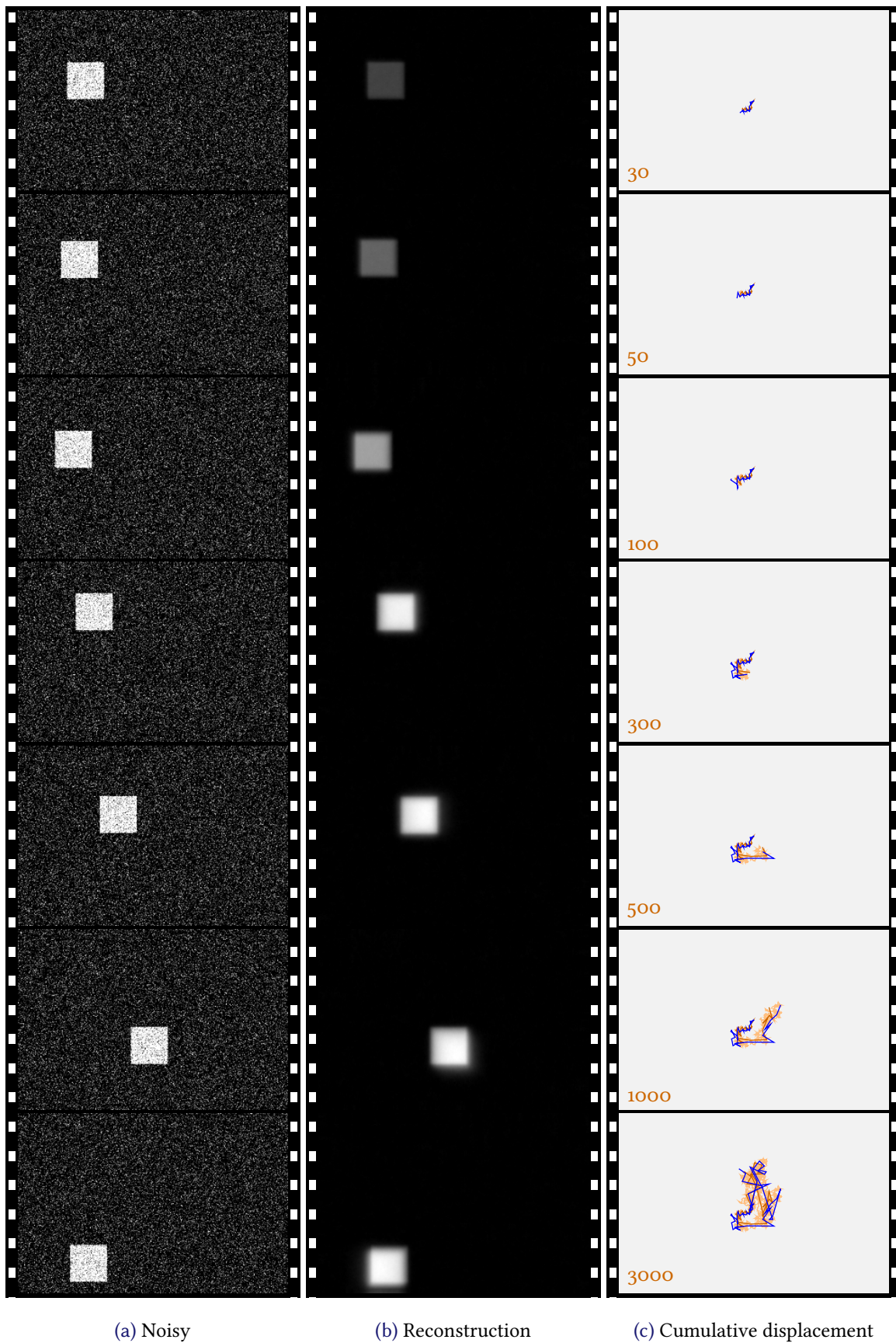


Figure 9: Square, POPD, unknown displacement, $\rho = 0$. The blue line in (c) indicates the estimated displacement field.

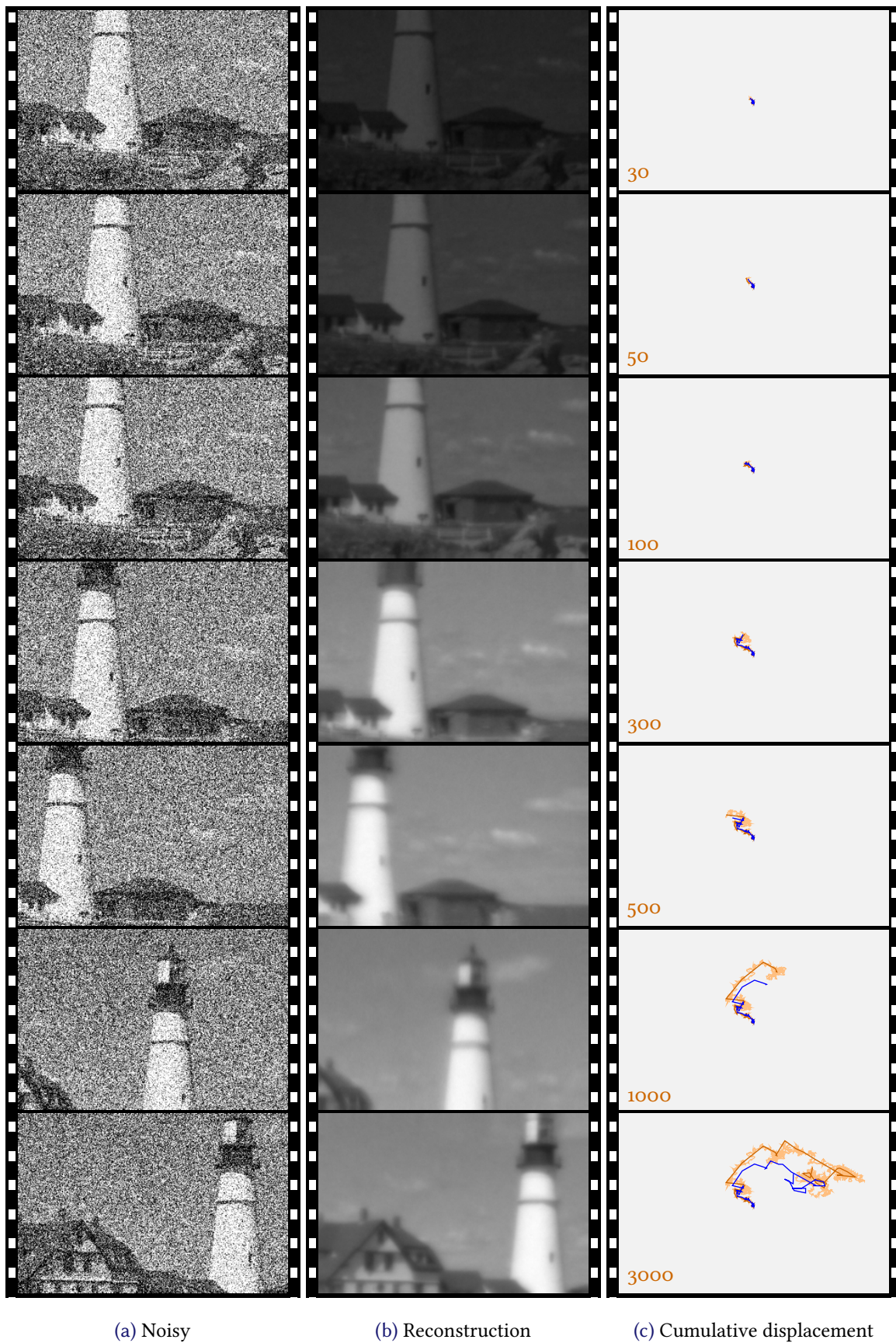


Figure 10: Lighthouse, POPD, unknown displacement, $\rho = 0$. The blue line in (c) indicates the estimated displacement field.

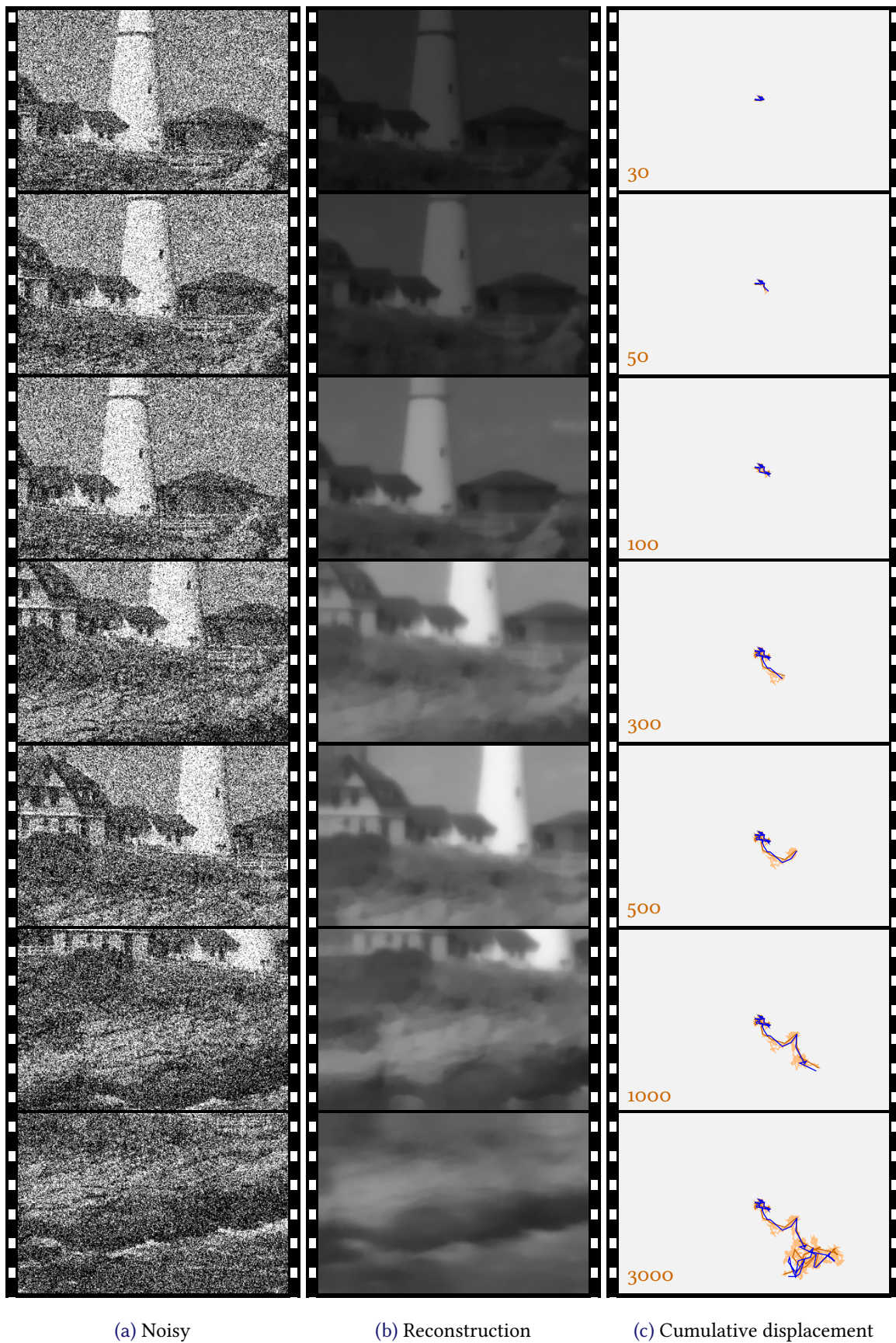


Figure 11: Lighthouse, POPD, unknown displacement, $\rho = 100$. The blue line in (c) indicates the estimated displacement field.